DEVELOPMENT OF A METHOD TO LOAD RATE GENERAL AVIATION AIRPORTS WITH ENVIRONMENTAL CONSIDERATIONS

A Thesis

By

GARRETT W. DORSETT

Submitted to the Graduate and Professional School of
Texas A&M University
in partial fulfillment of the requirements for the degree of

MASTER OF SCIENCE

Chair of Committee,	Charles Gurganus
Co-Chair of Committee,	David Allen
Committee Members,	Mark Everett
Head of Department,	Sharath Girimaji

May 2023

Major Subject: Ocean Engineering

ABSTRACT

Aerial transportation infrastructure is vital to connecting communities across the United States and the globe. It provides critical support functions in transporting purchased goods and resources, providing access to medical treatment, allowing timely travel for businesses, and strengthening national security. General aviation (GA) airports make up the vast majority of the total number of airports in the country and, while vital to the national economy, primarily serve communities through specialized roles. Due to the volume of GA facilities, they are more accessible to suburban and rural communities thus providing an opportunity to offer emergency response to these populations. However, the Federal Aviation Administration (FAA) design and maintenance specifications regarding GA airports are non-specific and do not reflect the differences in the use and funding of these airports. Therefore, GA airport traffic levels and runway structural capacities are not clearly defined under FAA guidelines. A misunderstanding of the pavement capability increases risk to large emergency aircraft in need of utilizing these airports.

This research seeks to develop a methodology to load rate GA airports with consideration for facilities located in coastal regions that are at greater risk of experiencing flood events. Procedures are developed to accurately estimate annual airport traffic and pavement structural capacity during normal and inundated conditions using conventional pavement test methods and FAA software. Results indicate that the proposed methodology is capable of producing accurate and repeatable load ratings for both normal and inundated pavement conditions.

DEDICATION

This thesis and associated work are dedicated to Jordan and Belle. Thank you both for your patience and support.

ACKNOWLEDGEMENTS

I would like to thank my graduate advisor and committee chair, Dr. Gurganus. I would also like to recognize my committee co-chair, Dr. Allen, and member, Dr. Everett.

Thank you also to my parents, and Mike and Carrie Rampy, for your encouragement, love, and support.

CONTRIBUTORS AND FUNDING SOURCES

Contributors

This research was supervised by a thesis committee consisting of Dr. Gurganus, advisor and committee chair, and Dr. Allen, co-chair, of the Department of Ocean Engineering, and Dr. Everett of the Department of Geophysics.

The airport testing plan and data used in sections 4-6 was collected by Mr. Lee and Tyler Gustavus, and Mr. Jason Huddleston of the Texas A&M Transportation Institute.

All other work pertaining to and contained in this thesis was completed by the student independently.

Funding Sources

Graduate study was supported by a scholarship from the American Bureau of Shipping, the Texas Aggie Graduate Grant from Texas A&M University, and the Texas A&M Transportation Institute.

NOMENCLATURE

AC	Advisory Circular
ACN	Aircraft Classification Number
ACR	Aircraft Classification Rating
BCI	Base Curvature Index
CDF	Cumulative Damage Factor
FAA	Federal Aviation Administration
FAARFIELD	Federal Aviation Administration Rigid and Flexible Iterative Elastic Layered Design
FWD	Falling Weight Deflectometer
GA	General Aviation
GPR	Ground Penetrating Radar
GVW	Gross Vehicle Weight
LWD	Lightweight Deflectometer
NASA	National Aeronautics and Space Administration
NDT	Non-Destructive Testing
PCN	Pavement Classification Number
PCR	Pavement Classification Rating
PI	Plasticity Index
SN	Structural Number
SWL	Single Wheel Load
TXGLO	Texas General Land Office

USDA	United States Department of Agriculture

TABLE OF CONTENTS

Page

LIST OF FIGURES

Page

LIST OF TABLES

Page

1. INTRODUCTION

Aerial transportation infrastructure is vital to connecting communities across the United States and the globe. The nation's system of airports provides critical support functions in transporting purchased goods and resources, providing access to medical treatment, allowing timely travel for businesses, and strengthening national security. There are over 19,000 facilities within the United States dedicated to aerial infrastructure [1]. These facilities support national economic stability and ensure the relevance of the nation on a global scale. Airports are classified into three main categories: commercial service, reliever, and general aviation (GA) airports. Commercial airports serve national and international economies, generate high passenger and cargo throughput, and experience heavy annual traffic. GA airports make up the vast majority of the total number of airports in the country and, while vital to the national economy, primarily serve communities through specialized roles.

The Federal Aviation Administration (FAA) is the federal entity over all aviation in the United States. The role of the FAA is to issue and enforce regulations and specifications regarding aircraft manufacturing, pilot training, aerial safety, and airport facilities. The FAA also controls and maintains funding for all airport facilities through the National Plan of Integrated Airport Systems and the Airport Improvement Program [1].

1.1. Problem Statement

Compared to commercial airports, GA airports experience less annual traffic, less passenger and cargo throughput, and are more accessible to communities and local businesses. GA airports may be owned, operated, and maintained by regional entities such as city governments. Many GA airports were constructed in the mid-20th century for military use. The

thin, flexible pavement sections utilized at these facilities are more vulnerable to heavier loads of modern aircraft. GA airports vary in size and capacity depending on the region they serve but are typically smaller than commercial airports. Because of this, GA airports are frequently used by hobby pilots, private charters, local commercial industries, and first responders for training, quick transportation, surveying, and emergency response, respectively.

Figure 1 displays the disparity between the number of commercial and GA airports in the state of Texas. This presents an opportunity for GA airports to provide resources for accelerated emergency response and illustrates the necessity for these facilities to be properly operated and maintained. For example, when hurricane Ian made landfall in the fall of 2022, communities in Florida and South Carolina were cut off from receiving essential medical supplies and aid. Local and national responders have the opportunity to use GA airports to evacuate residents and distribute aid to communities that are difficult to access during climate emergencies. However, the FAA design and maintenance specifications regarding GA airports are non-specific and do not reflect the differences in the use and funding of these airports. Therefore, GA airport traffic levels and runway structural capacities are not clearly defined under FAA guidelines. Misunderstandings of the pavement capability increases risk to large emergency aircraft in need of utilizing these airports.

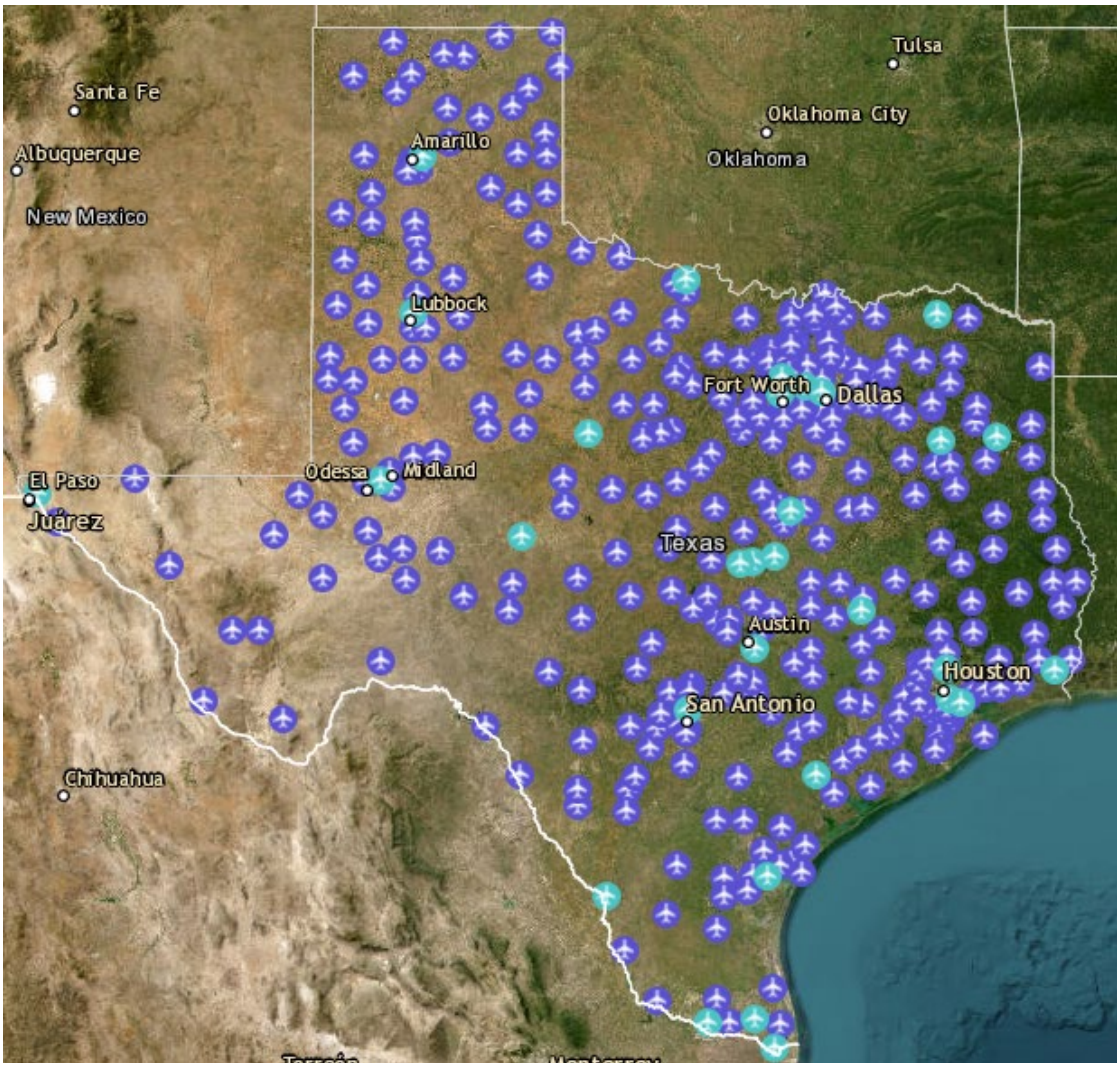

Figure 1. Texas Airport Directory Map of Commercial (blue) and GA (purple) Airports. Reprinted from [2]**.**

The purpose of this research is to develop a methodology to load rate GA airports with consideration for facilities located in coastal environments that are at greater risk of experiencing climate (flood) events as shown in Figure 2. GA airports in such an environment must perform the same functions as inland facilities but are also subjected to more extreme weather events that

can inundate the runway pavement layers and expedite pavement structural deterioration [3]. In this research, procedures are developed to accurately estimate the annual traffic of an airport and rate the structural capacity of the runway using non-destructive testing (NDT) and FAA software. A flood event is simulated to determine how water inundation of the pavement subsurface layers impacts the allowable load of the pavement during and immediately after a flood event. The results of the developed procedures will provide GA airport managers and owners with information on the aircraft loads the airport facility can sustain under normal operating conditions and under extreme weather conditions.

Figure 2. Wharton Regional Airport (ARM) Flooding in the Aftermath of Hurricane Harvey in 2017.
Reprinted from [4]**.**

1.2. Literature Review

A literature review was conducted to better understand

- the design and construction practices surrounding airport pavements
- the impact of climate events on pavement strength and structural integrity
- how the subsurface material interacts with moisture.

Literature regarding airfield pavements suggested that design specifications are too vague to accurately serve the wide variety of airports within the country. Pavements are rated based on the subgrade materials, but evaluation of the in-service pavement is based primarily upon visual inspection, not the subsurface conditions of the pavement structure [5].

Pavement flood resilience is dependent on the construction quality and the period of inundation during climate events. Pavement strength metrics were found to have recovered shortly after flooding, with the drying of the base layer contributing the most to overall pavement strength, but the pavement service life is adversely affected with each event. The subsurface material response to flooding indicated that the saturation levels of the soil are related to the material strength. Literature found that moisture damage to infrastructure is a result of soil expansion and shrinkage during the saturation and drying process associated with flooding.

1.2.1. Airport Pavement Design and Evaluation

The FAA provides specifications and regulations to the nation's system of airports (both commercial and GA) through reports called Advisory Circulars (AC). These documents are typically distributed on an as needed basis to replace previous AC notices with new specifications. For this research, ACs and manuals relating to GA airports constructed using highway pavement materials were utilized.

Many commercial and large GA airports build runways and associated roadways using rigid pavement materials. Rigid pavements can withstand greater loads and require less maintenance over their life. However, because they are much more expensive to construct and there are fewer maintenance options available when the need arises, most GA airports utilize flexible pavement runways. Given that there is a tradeoff in strength, the FAA limits the use of flexible pavement (highway materials) to GA airports that serve aircraft under 60,000 pounds. The AC specifying the use of flexible pavement also includes language to ensure that safety and service life are not negatively impacted [6]. This specification represents the only distinction that was found in the literature between the design of GA and commercial airport pavements.

FAA pavement design specifications depend upon the gross vehicle weight (GVW) of the aircraft. As such, there is a need to accurately determine if a particular aircraft is allowed to land at an airfield without causing the runway to fail prematurely as in Figure 3. In the past, this has been accomplished via the Aircraft Classification Number (ACN) and the Pavement Classification Number (PCN). The ACN value is calculated by aircraft manufacturers using the GVW of the aircraft and the landing gear configuration. The PCN value is calculated for an airport based on the category of the pavement subgrade. If the ACN of an aircraft is less than the PCN of the airport, the aircraft is allowed to land without restrictions. If the ACN is greater than the PCN, then the aircraft's weight must be restricted to land at the airport. In this way, the ACN/PCN system evaluates the amount of damage a pavement experiences under an aircraft load by measuring the proposed subgrade deflection [7].

a) b)

Figure 3. Olney Airport (ONY) a) Rutting and b) Rutting and Surface Cracking.

In the past 10 years, the FAA has moved away from the ACN/PCN system to the Aircraft Classification Rating (ACR) and Pavement Classification Rating (PCR) system. The ACR/PCR system represents an improvement over ACN/PCN in that layered elastic analysis is used to predict the pavement mechanical response to loading, all aircraft wheels are considered within the pavement response calculation, and the characteristics of new paving materials are considered [8], [9]. The ACR/PCR system is reported in a manner similar to the ACN/PCN rating. The ACR of a certain aircraft is measured and compared to the PCR of an airport's pavement. So long as the ACR is less than the PCR, the aircraft is cleared for unrestricted operations at that airfield [10].

1.2.2. Impact of Flood Events on Pavement Strength

Literature exploring the impact of flood events on pavement strength found that construction and the saturation of the base and subgrade layers were the most important factors

in determining the strength and remaining service life of pavements exposed to climate events [11], [12]. During flood events, thin, flexible pavements were found to be the most vulnerable to damage, while rigid pavements with thick surface courses were the most resistant. This resulted in pavements designed for low traffic volumes experiencing greater damage and strength reduction compared to high traffic pavements [11], [13].

Literature also studied the lasting effects of flood events on pavement. During the event, pavement structural capacity was reduced by as much as 70%, but when tested shortly after the event, structural capacity was found to have recovered to within 30% of the designed strength [11], [12], [14]. Although literature found that soil properties begin to return to in-situ states just days after a flood event, the rate at which the pavement regained structural capacity was found to be dependent upon the inundation of the base and subgrade layers, and the subgrade material. The overall strength of pavements after flooding was found to be closely tied to the state of the base layer. Results showed that, while pavements lose significant structural capacity when the unbound material layers are submerged, strength is rapidly regained once the subsurface water level reaches the interface of the base and subgrade layer [11], [15], [16].

The structural deficiencies incurred from flood events lessened the pavement service life. The natural deterioration of the pavement surface and structure was found to be expedited by water inundation, with flood events effectively removing a year from the pavement life [17], [15]. Saturation effects within the pavement subsurface materials resulted in unrecoverable damages that reduced the pavement structural number (SN) and subgrade modulus up to 18% and 26%, respectively [16].

1.2.3. Soil-Moisture Interaction

Important soil properties in pavement construction are the resilient modulus (M_r), and the degree of saturation. The resilient modulus of a soil is an indication of the material's strength, while the degree of saturation indicates the relative level of moisture within the void space of a soil. Previous studies have shown the resilient modulus of a soil is controlled by the degree of saturation [18]. Research has shown that the resilient modulus is inversely related to the degree of saturation and moisture content [19], [20]. This relationship was crucial in defining the structural strength, damage, and remaining life of pavements and subgrade soils that had undergone climate events (saturation) [21], [14]. Literature reviewed for this research intended to better understand this relationship by first determining reliable methods for calculating both properties, then experimenting to determine the true effect the degree of saturation has on the resilient modulus of a soil.

Resilient modulus is a physical property of a material, and in pavement engineering, gives an indication of the strength of the material. The resilient modulus is traditionally calculated in a laboratory setting using AASHTO T 307-99 standard specifications. Literature found that Equation 1 [20], produced by the Mechanistic-Empirical Design Guide, yielded acceptable modulus values expressed as a function of the bulk and octahedral stresses. Research also related the soil index properties and unconfined compression results to the resilient modulus, shown in Equation 2 [18].

$$M_R = k_1 P_a * \left(\frac{\theta}{P_a}\right)^{k_2} * \left(\left(\frac{\tau}{P_a}\right) + 1\right)^{k_3} \quad (1)$$

Where

Mr = resilient modulus

θ = bulk stress

τ = octahedral shear stress

k1, k2, k3 = model parameters

$$M_r = 45.8 + 0.00052 * \frac{1}{a} + 0.188 q_u + 0.45 PI - 0.2166 \gamma_d - 0.25 S - 0.15 P_{200} \quad (2)$$

Where

M_r = resilient modulus

a = initial tangent modulus of a stress-strain curve from UC test

q_u = UC strength

PI = plasticity index

γ_d = dry unit weight

The in-situ degree of saturation can be calculated empirically from Equation 3 [22], where the moisture content is dependent upon the soil properties and moisture content within the sample.

$$S = \frac{w}{\frac{\gamma_w}{\gamma_d} - \frac{1}{G_s}} \quad (3)$$

Where

S = in-situ saturation

w = moisture content

γ_w = unit weight of water

γ_d = dry unit weight

G_s = specific gravity

The in-situ degree of saturation is useful in predicting the structural state of the in-situ material. However, to compare in-situ to optimum material properties, the optimum degree of saturation is calculated as shown in Equation 4 [23]. Knowledge of both the optimum and in-situ resilient modulus and degree of saturation values gives an indication of the subsurface structural integrity under different climate conditions.

$$S_{opt} = \frac{\frac{w_{opt} * \gamma_{d\max}}{\gamma_{water}}}{1 - \frac{\gamma_{dmax}}{\gamma_{water} * G_s}} \quad (4)$$

Where

W_{opt} = optimum moisture content determined from AASHTO tests

γ_{dmax} = maximum dry density of the material

γ_{water} = unit weight of water

G_s = specific gravity

Literature provided two different models to relate the material resilient modulus to the moisture properties captured by the degree of saturation. For a given optimum resilient modulus and known change in degree of saturation, Equation 5 [24] illustrates a linear relationship between resilient modulus and saturation.

$$M_{r_{wet}} = M_{r_{opt}} + \left(\frac{dM_r}{dS}\right) * \Delta S \quad (5)$$

Where

M_{rwet} = resilient modulus at increased saturation

M_{ropt} = resilient modulus at the optimum moisture content

dMr/dS = gradient of the resilient modulus with respect to the saturation

ΔS = change in degree of saturation

The Mechanistic-Empirical Design Guide also suggested Equation 6 be used to model the relationship for soils. This model included the effect of plasticity index (PI), a soil property that describes the reaction of soils with moisture. Due to this inclusion, Equation 6 [20] was found to have a large amount of variability, and the literature suggested that the model may not accurately represent all soil types.

$$\log\left(\frac{M_R}{M_{Ropt}}\right) = a + \frac{(b-a)}{1+\exp\left[ln\left(-\frac{b}{a}\right)+k_m*(S-S_{opt})\right]} \quad (6)$$

Where

M_r = resilient modulus at any degree of saturation

M_{ropt} = resilient modulus at a reference condition

a = minimum of log term

b = maximum of log term

S - S_{opt} = variation in degree of saturation expressed in decimals

$k_m = 0.362*PI + 3.545$

Soil suction, like PI, is a property of soils that is used to describe the interaction of soil and moisture. Soil suction is the magnitude of negative pore water pressure within the soil and can be used to calculate the water content of in-situ material. Soil suction can be calculated by Equation 7 [19] in which the relative humidity within a soil sample is considered. Equation 8

[25] was used to determine the shear strength of the material. It was found that the magnitude of suction was dependent on both the water content and degree of saturation of the soil.

$$h_t = -\frac{RT}{v_w} * \ln\left(\frac{p}{p_0}\right) \quad (7)$$

Where

h_t = total suction

R = ideal gas constant

T = absolute temperature

v_w = volume of a mole of liquid water

p = water vapor pressure

p_0 = saturated water vapor pressure

Literature identified soil suction as one of the critical factors in determining the behavior of expansive soils. Expansive soils are clay soils that have high PI and linear shrinkage values. These soils are prevalent in many parts of the world, but laboratory strategies that effectively minimize expansion are not translated to field construction. Therefore, differential soil expansion (heave) is a major issue that causes premature failure of pavements, as shown in Figure 4 [26], [27].

$$\boldsymbol{\tau = c + \sigma_n * tan\phi} \quad (8)$$

Where

τ = shear stress

c = soil cohesion

σ_n = net normal stress at failure on the failure plane

ϕ = angle of internal friction

Figure 4. Roadway Damage Due to Flooding in Iowa. Reprinted from [14]**.**

2. NON-DESTRUCTIVE TESTING (NDT) METHODS

Non-destructive testing (NDT) is testing that does not damage the pavement surface or structure. The NDT methods used to conduct this research are the same methods used by transportation agencies for network pavement management systems. NDT is preferred over destructive testing, as the process is less invasive, requires less traffic control, and yields useful data to assist agencies in project and network level developments. The following sections (2.1-2.4) define NDT methods and tools commonly used by TxDOT and other transportation agencies on highway pavements. Section 2.5 describes the use of airport-specific design software within this research.

2.1. Ground Penetrating Radar (GPR)

Ground penetrating radar (GPR) is a tool used by TxDOT and other research organizations to determine the pavement structure and locate subsurface defects. GPR is a mobile device that consists of a radar antenna fixed to the front of a moving vehicle as shown in Figure 5. The antenna sends and receives electronic pulses and reflections to determine pavement structure properties.

Figure 5. Ground Penetrating Radar Unit.
Reprinted from [28]**.**

The reflected signals occur at layer interfaces within the pavement, such that operators are able to determine the layer thickness using the vehicle speed. Because GPR signals are electrical, the conductivity of materials effects the strength of the reflected signal. This relationship makes GPR particularly useful in determining the location of moisture related defects such as stripping or voids within the pavement structure [29]. For the purpose of this research, GPR was used to determine the pavement layer thickness for each of the tested airports. GPR was also used to identify areas of localized structural deficiencies within the pavement.

2.2. Falling Weight Deflectometer (FWD)

Falling weight deflectometer (FWD) is a mobile pavement testing system used by TxDOT that measures the deflection of pavement under a load. FWD systems as in Figure 6 consists of seven deflection sensors spaced one foot apart, starting at the load center.

Figure 6. Falling Weight Deflectometer.
Reprinted from [28]**.**

The FWD uses a 9,000 pound load dropped onto the pavement to produce a load impulse. The impulse creates a deflection bowl, depicted in Figure 7, in the pavement that is measured by the on board sensors. The raw deflection data from the sensors give a description of the pavement structural strength. The maximum deflection describes the surface strength, the deflections measured 12-24 inches from the load center describe the base/subbase layer strength,

and the deflections furthest from the load center describe the subgrade. However, pavement structural properties such as modulus (E) are determined through a backcalculation process. Backcalculation is performed through a software called MODULUS that uses the pavement temperature, layer thicknesses, and FWD deflection data as inputs. The output of the backcalculation procedure are the layer moduli values that can be used to calculate other pavement structural metrics and the pavement remaining life when used in conjunction with traffic data.

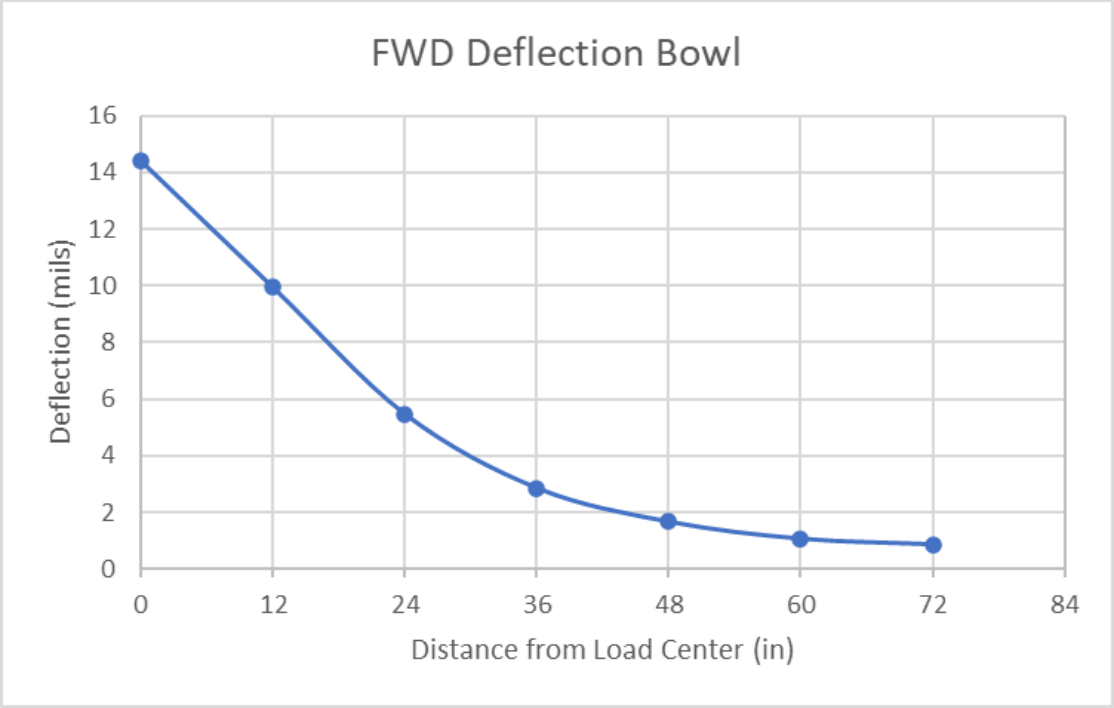

Figure 7. Deflection Bowl Generated from FWD Data.

For this research, FWD testing was done at every airport that was evaluated. FWD data was taken at regular intervals along the runways, taxiways, and associated pavements around the airfield to ensure the data collected was representative of the entire facility. The collected data were used to identify localized areas of potential failure and was used in conjunction with GPR to evaluate specific areas of interest for the airport managers. The backcalculated moduli values were used as the inputs for design software involved in the load rating process.

2.3. Lightweight Deflectometer (LWD)

Lightweight deflectometer (LWD) is a portable testing system that allows for the measurement of pavement strength. LWD tests are conducted by dropping a small load onto the pavement and measuring the induced deflections. The magnitude of the deflections gives an indication of pavement strength and are used to calculate the layer moduli values using Equation 9 [30]. The LWD consists of a 22 pound weight that is dropped along a shaft to impact a 12 inch metal plate resting on the pavement surface. The resulting deflections are measured in micrometers by three sensors on the pavement surface.

$$E = \frac{2\,\mathrm{Pr}(1-\nu^2)}{D_0} \tag{9}$$

Where

E = layer modulus

P = maximum contact pressure

r = plate radius

ν = Poisson's ratio for the selected layer

D_0 = deflection at the load center (maximum deflection)

Because of its similarity to existing FWD systems, extensive research has been performed to compare the results to FWD and identify the strengths and weaknesses of LWD. Research has found that LWD measurements provide similar pavement structural metrics, such as structural number, as FWD on flexible pavements [31] [32]. This research also found that LWD calculated resilient modulus values for the pavement subgrade trended with laboratory calculated values and the layer moduli values (E) could be related to resilient modulus calculated from FWD by Equation 10 [33].

$$M_{r_{FWD}} = 0.97E_{LWD} \quad (10)$$

Research testing with LWD has also proven that the system can characterize the material strength during the construction process and during periods of moisture inundation. Due to the cyclic loading nature of LWD, the material is compacted to similar levels as construction such that the results of the LWD test are congruent with the actual material properties, regardless of the testing conditions [30] , [34]. The capability of LWD to determine pavement health in various environmental and compaction conditions extends to traffic loading as well, as LWD has been found to accurately determine pavement deterioration from sustained traffic loading [35]. For the purpose of this research, LWD data was collected and compared to FWD data at one airport but was not utilized in the backcalculation process.

2.4. Federal Aviation Administration Rigid and Flexible Iterative Elastic Layered Design (FAARFIELD)

The Federal Aviation Administration Rigid and Flexible Iterative Elastic Layered Design (FAARFIELD) software is a program used to compute airport pavement thickness design using procedures developed by the FAA and distributed in AC documents. FAARFIELD utilizes a

mechanistic-empirical design procedure to determine important pavement metrics for both flexible and rigid pavements. The FAARFIELD software represents an advancement in airport pavement design in that the program has been modernized and the designs generated by the software are designed for fatigue failure of the pavement [36]. Design for fatigue failure is accomplished through the use of a cumulative damage factor (CDF) given by Equation 11 [6]. The CDF is the damage contribution of each aircraft within the traffic mix of an airport to the pavement such that the sum of all the CDF values for each aircraft in a given traffic mix is the total damage inflicted upon the pavement [37]. This concept is explained graphically by Figure 8. By using this method, engineers are able to determine the aircraft that cause the greatest damage to the pavement.

$$CDF = \frac{\text{number of applied repitions}}{\text{number of allowable repititions to failure}}$$

$$= \frac{(\text{annual departures}) * (\text{life in years})}{(\text{pass to coverage ratio}) * (\text{coverages to failure})}$$

$$= \frac{\text{applied coverages}}{\text{coverages to failure}} \tag{11}$$

Where coverage refers to a gear passing over and inducing a maximum load upon the pavement, and the pass to coverage ratio is the ratio of aircraft landing operations to a single gear producing load (coverage) upon a specific pavement location. Traditionally, the number of passes is different than the number of coverages due to aircraft wander across the pavement, but the pass to coverage ratio within this research is assumed to be one (i.e., every aircraft lands/taxies over the same location on the pavement) [38].

For the purpose of this research, FAARFIELD is used to define a representative traffic mix, calculate the pavement life under the associated traffic mix, and calculate the corresponding PCR for the pavement structure/traffic mix combination. The PCR value is reported as shown in Table 1 and consists of a numerical value, followed by codes representing the pavement type, subgrade category, tire pressure category, and the procedure used to determine the numerical PCR value.

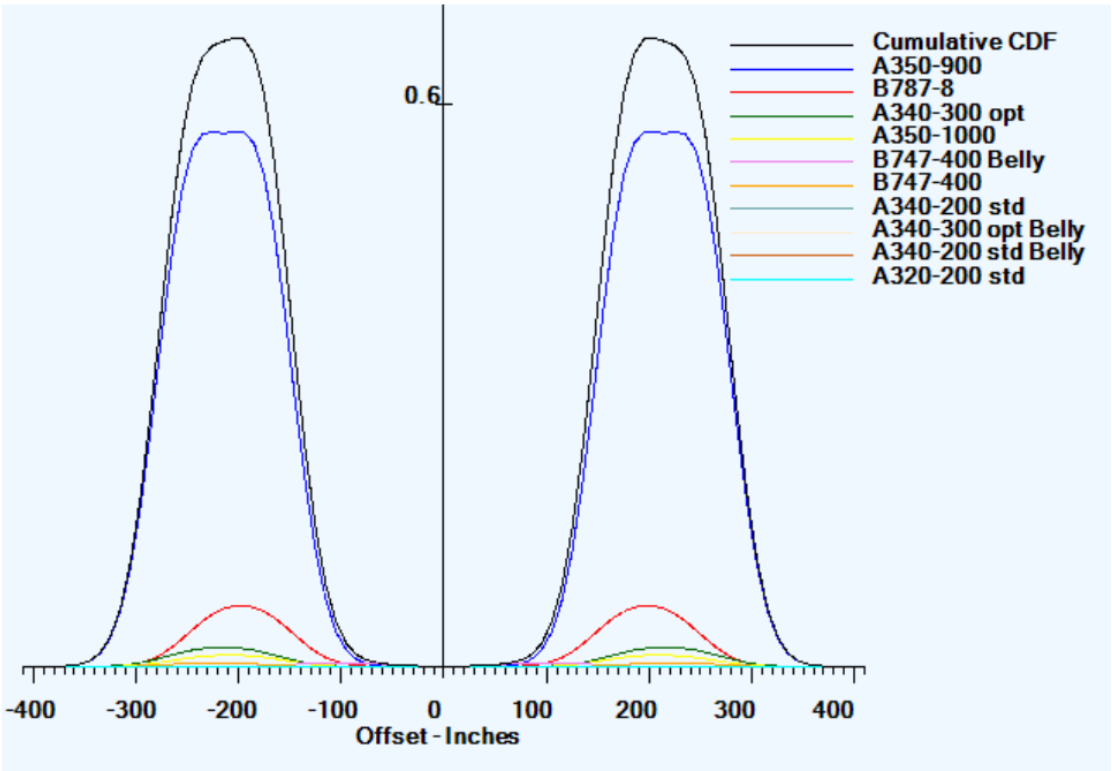

Figure 8. Example CDF Curve from FAARFIELD.

There are two procedures that can be used to determine the PCR value, technical evaluation or using aircraft. The technical method requires information about the traffic mix and the pavement layer thickness and material properties to compute the maximum ACR for the pavement. This ACR value is reported as the pavement PCR. To evaluate the PCR using aircraft, the largest ACR value within a given traffic mix is used as the PCR value [10].

Table 1. PCR Reporting Values.

Example PCR	345/F/B/X/T		
Numerical Value	Load carrying capacity of the pavement in terms of a single wheel load at tire pressure = 218 psi		
Pavement Type	Flexible (F) or Rigid (R)		
Subgrade Category	**Category**	**Modulus Range (psi)**	**Code**
	High	≥ 21,756	A
	Medium	14,504 – 21,756	B
	Low	8,702 – 14,504	C
	Ultra Low	< 8,702	D
Tire Pressure Category	**Category**	**Limit (psi)**	**Code**
	Unlimited	None	W
	High	≤ 254	X
	Medium	≤ 181	Y
	Low	≤ 73	Z
Method	Technical (T) or Using Aircraft (U)		

3. RESEARCH SCOPE

This research seeks to develop a practical and effective method to load rate GA airports such that environmental conditions are considered. By accomplishing this, the safety and effectiveness of GA airports will be increased as airport operators and managers will better understand the structural capacity of the airport pavement and use this to make informed decisions regarding the airport's ability to service incoming aircraft. The following sections (3.1-3.2) are necessary to better define the target facilities of this research.

3.1. General Aviation (GA) Airports

Over time, the functions of GA facilities have evolved to fill social and communal roles, and presently there is a wide variety of GA airport sizes, functions, and capabilities. To better define GA airports and make informed funding decisions, the FAA groups GA airports into one of the four categories listed in Table 2 [1].

Table 2. FAA General Aviation Airport Categories.

Category	Number of Facilities	Function
National	84	Community access to national and international markets.
Regional	467	Community access to statewide and interstate markets.
Local	1,236	Community access to intrastate markets.
Basic	668	Emergency, charter, and cargo service access to communities; flight training and personal flying.

Depending on their primary function, GA airports may have rigid, flexible, or grass turf airfields. Traffic control, if any, may be done through a tower or manager's office, and traffic may range from less than 100 to over 100,000 annual operations. National FAA specifications do not account for the differences in capabilities and traffic of every GA airport. Similarly, national funding opportunities may limit unique maintenance operations for GA airports in favor of standardized strategies. For this reason, it is necessary to develop a load rating method that accounts for specific loading and environmental effects.

3.2. Coastal Environments

To better understand which GA airports are more prone to damage from climate events, the term, "coastal environment" was defined. The Texas General Land Office (TXGLO) defines a coastal environment geographically within the coastal management program as all or part of any state county bordering the Gulf of Mexico, as illustrated in Appendix A [39]. Additionally, the National Aeronautics and Space Administration (NASA) defines a low-elevation coastal zone as an area located at an elevation of 65 feet or less above sea level [40]. These defined regions often play important environmental roles in sustaining the coastline and may be subjected to harsher environmental conditions such as storm surge and flooding [3]. In total, data from 10 GA airports was collected for this research as shown in Figure 9. Of these, seven were classified as being located in a coastal area under the TXGLO and/or NASA and prone to flooding during a climate event.

Figure 9. Locations of Tested Airports Relative to TXGLO Coastal Boundary.

4. LOAD RATING METHODOLOGY

The following sections (4.1-4.2) outline the proposed methodology used to load rate GA airports. The main tool used in the procedure is FAARFIELD, as the program utilizes FAA definitions to define and identify the failure of a runway pavement. The procedure requires runway material and structural inputs, as well as estimated traffic levels to estimate the PCR and remaining life of the runway.

4.1. General Aviation Airport Traffic Classifications

GA airports are categorized by the FAA into four categories depending on the community served by the airport [1]. These categories allow for an interconnected system of GA airports that work in conjunction to serve the nation, but these categories do not address the traffic loads experienced by the airfields. An important input for the FAARFIELD design software is the annual traffic. Annual traffic refers to the number of annual takeoff operations, regardless of aircraft GVW and size, at a given airport. It was found in this study that GA airports have very little information regarding airport traffic. In general, airport managers were aware of the average aircraft size and had a good understanding of when the airport would experience more or less daily traffic, but accurate annual traffic values and historical traffic records were not available. Annual traffic values used to generate GA traffic classes were accessed through AirNav.com, a website that provides airport and travel information for pilots [41].

There are 266 airports in the state of Texas that are classified by the FAA as GA airports. Using AirNav, annual traffic values for 192 of these facilities were used to generate a distribution with a mean of 18,200 operations and a standard deviation of 24,853 operations. The

histogram plot in Figure 10 consists of four bins, denoting four traffic categories. The left skewed shape of the normal distribution was used to inform the bin sizes of the histogram. The average annual traffic values for each of the four traffic categories are given in Table 3. Because these GA classes are defined in terms of annual traffic instead of regional influence, they can be used to develop traffic mix inputs for FAARFIELD design applications.

Table 3. Traffic Category Average Annual Traffic Values.

Traffic Category	Average Annual Traffic Operations
1	2,469
2	10,990
3	28,803
4	75,774

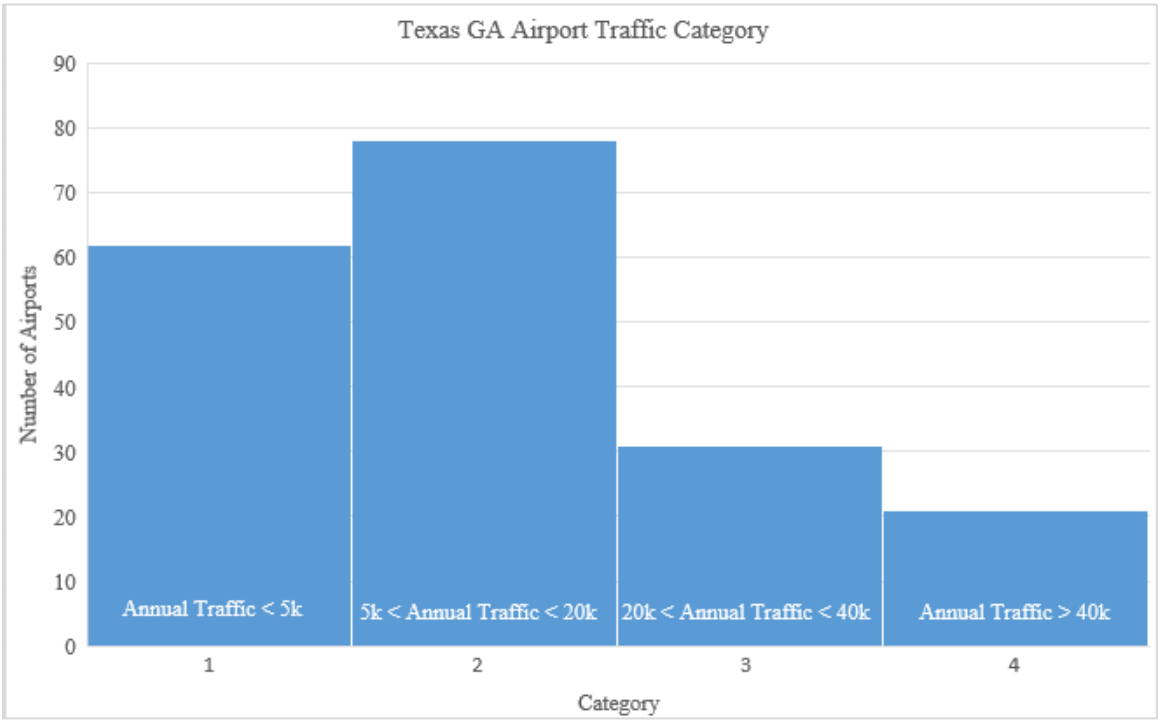

Figure 10 . Texas GA Airport Traffic Categories.

4.1.1. Design Traffic Mix

One of the inputs for the FAARFIELD program is a design traffic mix that includes aircraft characteristic data such as GVW, tire pressure, and tire contact area. The traffic mix is necessary as the program uses the applied loading from the mix to evaluate the structural performance of the pavement. Additionally, FAARFIELD permits the user to adjust the annual operations over the pavement life for each aircraft from the traffic mix window as shown in Figure 11. This feature was used considerably to manipulate the loads applied to the pavement structure over its service life.

Given that there are four distinct GA airport categories based on the amount of annual traffic, it is necessary to define four traffic mixes within FAARFIELD to accurately represent the loads experienced by airports. The FAARFIELD program has an extensive vehicle library for users to create a design traffic mix, as well as a user defined vehicle option that allows for the creation of a specific design vehicle. However, given the lack of traffic data from many GA airports, it was necessary to research common consumer aircraft to generate realistic traffic mixes. For example, a rural GA airport in the first traffic category (less than five thousand annual departures) is not likely to accommodate a large private jet, but instead may commonly host small hobby planes. However, a GA airport in the third category is likely to have large, heavy jets in addition to hobby craft in the traffic mix.

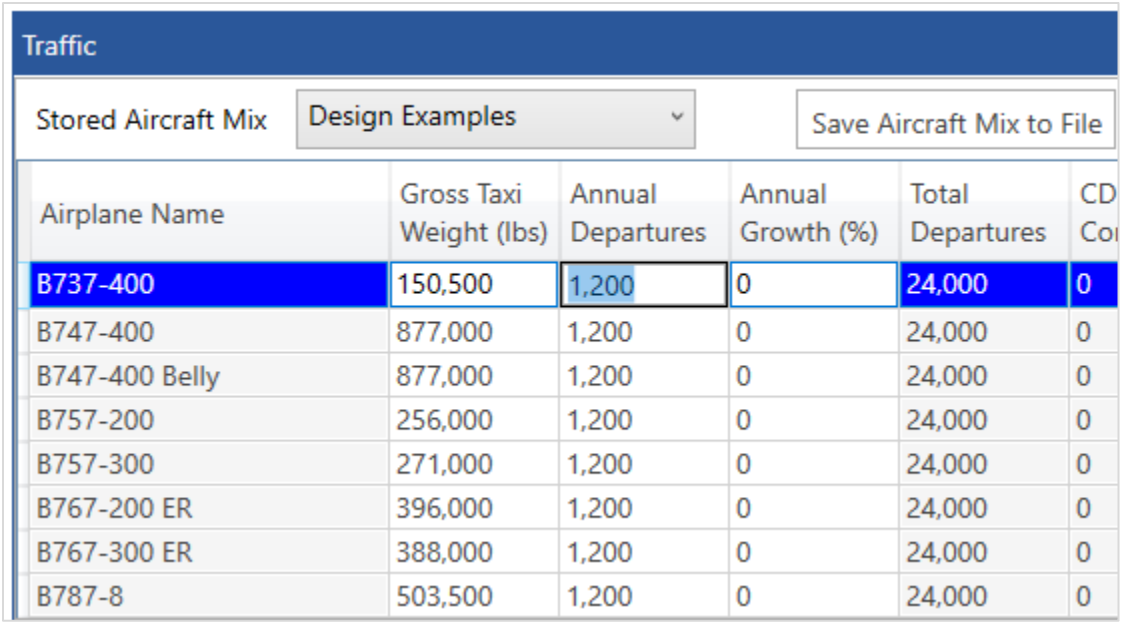

Airplane Name	Gross Taxi Weight (lbs)	Annual Departures	Annual Growth (%)	Total Departures	CD Co
B737-400	150,500	1,200	0	24,000	0
B747-400	877,000	1,200	0	24,000	0
B747-400 Belly	877,000	1,200	0	24,000	0
B757-200	256,000	1,200	0	24,000	0
B757-300	271,000	1,200	0	24,000	0
B767-200 ER	396,000	1,200	0	24,000	0
B767-300 ER	388,000	1,200	0	24,000	0
B787-8	503,500	1,200	0	24,000	0

Figure 11. Adjusting Aircraft Annual Departures in the FAARFIELD Traffic Interface.

4.1.2. Generating Traffic Mixes

A representative traffic mix was generated for each traffic category by comparing characteristics of popular aircraft to characteristics of the GA airports in each category and the communities they serve. The aircraft models used in each of the traffic mix were selected using sales information provided on General Aviation News' website shown in Table 4. The website included lists of the ten best-selling piston, turboprop, and jet engine aircraft in 2020 [42], [43], [44]. The selected aircraft were extracted from the FAARFIELD vehicle library, and if the exact model was unavailable, either a similar aircraft was substituted or the aircraft was modelled using the user defined vehicle function if the aircraft specifications were publicly available.

Table 4. Best-Selling Aircraft 2020 from General Aviation News.

Piston Aircraft	Turboprop	Jet Engine
Cessna Skyhawk 172S	Pilatus PC-12	Gulfstream 500-650
Cirrus SR22T	Cessna Grand Caravan	Cirrus SF50 Vision
Piper Archer III	Air Tractor AT-802A	Bombardier Global
Diamond DA40	Daher TBM 940	Embraer Phenom 300
Cirrus SR22	Beechcraft King Air 350i	Bombardier Challenger
Diamond DA42	Piper M600	Pilatus PC-24
Tecnam P2008	Air Tractor AT-502B	Dassault
Cirrus SR20	Beechcraft King Air 250	Hondajet
Flight Design CT	Air Tractor AT-502A	Cessna Citation Latitude
Tecnam ASTM LSA	Air Tractor AT-402B	Cessna Citation M2

In general, piston aircraft are the cheapest aircraft available to the consumer market, while jet engine aircraft are the most expensive. For this reason, the annual traffic values are skewed to include more piston aircraft than jet engine in each of the traffic mixes. Annual departures for each aircraft model included in the overall traffic mix increased with each traffic category except the included Air Tractor model. This is because Air Tractor produces aircraft for agricultural and emergency response uses, so it was unlikely that traffic operations would increase for this model even though it is widely available. Additional review of the airport websites indicated that airports with over 40 thousand annual departures operate some commercial flights in addition to private flight operations [45], [46], [47]. This necessitated the fourth GA airport category, in which two commercial jets, the Boeing 737 and Airbus A321, used by American, Southwest, and United Airlines are included in the traffic mix [48], [49] [50]. Given the data and assumptions provided through aircraft research, the following Tables 5-8 list the traffic mix for each GA airport category. For categories 1-3, annual traffic totals for each

aircraft were designed in such a way that most traffic are piston aircraft, while jet engine aircraft contribute the least to the annual traffic to best reflect actual traffic patterns. The total number of operations from all the aircraft included in the mix is approximate to the average traffic value for that category.

Table 5. Category 1 Design Traffic Mix.

Aircraft	Annual Departures	Engine
Cessna 172 Skyhawk	300	Piston
PA-28R-200 Cherokee Arrow	300	Piston
Cirrus SR22T	300	Piston
Diamond DA40	300	Piston
Tecnam P2008	300	Piston
Cirrus SR20	250	Piston
Flight Design CT	250	Piston
Tecnam ASTM LSA	250	Piston
Cessna 208B Grand Caravan	200	Turboprop
Beechcraft King Air 300	25	Turboprop
Beechcraft King Air 350	25	Turboprop
AT-802A	5	Turboprop
Annual Traffic	**2,505**	

Table 6. Category 2 Design Traffic Mix.

Aircraft	Annual Departures	Engine
Cessna 172 Skyhawk	1050	Piston
PA-28R-200 Cherokee Arrow	1050	Piston
Cirrus SR22T	1050	Piston
Diamond DA40	1050	Piston
Tecnam P2008	1050	Piston
Cirrus SR20	950	Piston
Flight Design CT	950	Piston
Tecnam ASTM LSA	950	Piston
Cessna 208B Grand Caravan	950	Turboprop
Pilatus PC-12	600	Turboprop
Beechcraft King Air 300	600	Turboprop
Beechcraft King Air 350	600	Turboprop
Cessna Citation II	60	Jet
Cessna Citation X	60	Jet
AT-802A	25	Turboprop
Annual Traffic	**10,995**	

Table 7. Category 3 Design Traffic Mix.

Aircraft	Annual Departures	Engine
Cessna 172 Skyhawk	2600	Piston
PA-28R-200 Cherokee Arrow	2600	Piston
Cirrus SR22T	2600	Piston
Diamond DA40	2600	Piston
Tecnam P2008	2600	Piston
Cirrus SR20	2400	Piston
Flight Design CT	2400	Piston
Tecnam ASTM LSA	2400	Piston
Cessna 208B Grand Caravan	2400	Turboprop
Pilatus PC-12	1500	Turboprop
Beechcraft King Air 300	1500	Turboprop
Beechcraft King Air 350	1500	Turboprop
Cessna Citation II	350	Jet
Cessna Citation X	350	Jet
Dassault Falcon 50	350	Jet
Bombardier CL-604	350	Jet
Gulfstream G550	350	Jet
AT-802A	25	Turboprop
Annual Traffic	**28,875**	

Table 8. Category 4 Design Traffic Mix.

Aircraft	Annual Departures	Engine
Cessna 172 Skyhawk	2600	Piston
PA-28R-200 Cherokee Arrow	2600	Piston
Cirrus SR22T	2600	Piston
Diamond DA40	2600	Piston
Tecnam P2008	2600	Piston
Cirrus SR20	2400	Piston
Flight Design CT	2400	Piston
Tecnam ASTM LSA	2400	Piston
Cessna 208B Grand Caravan	4500	Turboprop
Pilatus PC-12	4500	Turboprop
Beechcraft King Air 300	5000	Turboprop
Beechcraft King Air 350	5000	Turboprop
Cessna Citation II	6500	Jet
Cessna Citation X	6500	Jet
Dassault Falcon 50	6500	Jet
Bombardier CL-604	6500	Jet
Gulfstream G550	6500	Jet
Boeing B737-700	2000	Jet
Airbus A321neo	2000	Jet
AT-802A	25	Turboprop
Annual Traffic	**75,725**	

4.2. Load Rating Procedure

The purpose of load rating an airport pavement is to determine the maximum allowable load the runway may sustain before failure. This information is useful in ensuring that airport operations are conducted in a safe and sustainable manner and in determining the service life of the pavement, even after years of service. This research developed two values pertaining to the load rating of airfield pavements: the load rating for repeated operations, and the single use load rating. The load rating for repeated operations is the maximum load an airport pavement can

withstand without compromising the 20-year service life. Alternatively, the single use load rating is the maximum load an airport pavement can withstand to safely conduct a single aircraft operation. The latter value is not intended to be used in determining the response under daily airport traffic, but instead for heavier emergency service and military aircraft used to transport personnel, supplies, and resources to areas in need of aid. Both the repeated operations and single use load rating procedures developed in this research utilize NDT and backcalculation methods to generate necessary inputs for use in the FAARFIELD design software.

4.2.1. Load Rating for Repeated Operations

After determining the traffic category of an airport using traffic data from AirNav and selecting the appropriate traffic mix, the pavement structure and traffic mix are entered into FAARFIELD. Once entered, a PCR report is generated for that specific pavement structure and traffic mix by selecting PCR analysis type and running the program. The PCR report includes PCR and ACR information, from which the critical, or design, aircraft is listed along with the maximum allowable GVW for the input pavement. The GVW for the critical aircraft is then divided by two to give the single wheel load (SWL) of the aircraft.

Some critical aircraft models may have a dual wheel gear configuration in which the SWL of the aircraft is a quarter of the GVW. However, the thinness of many GA pavement structures is such that the dual wheels are spaced too close together to behave like two wheels. Therefore, the GVW is divided by two regardless of the landing gear configuration of the critical aircraft. In this way, the load rating figure remains accurate for single wheeled gear, and conservative for dual wheel gear such that a factor of safety is developed within the procedure.

The SWL value calculated from the traffic critical aircraft is representative of an unchanging traffic mix. To use this value as the load rating for repeated operations would result

in traffic being limited to the traffic mix accompanying the airport category, and not representative of actual traffic. Real world traffic patterns mirror the health of local and national economies. As shown by Figure 12, the potential for increases in annual traffic requires that the load rating for repeated operations be more robust. Therefore, the calculated SWL from the traffic mix is used to estimate the maximum allowable SWL over the entire service life of the pavement, and in doing so, the pavement is loaded and damaged by only operating the critical aircraft for the life of the pavement.

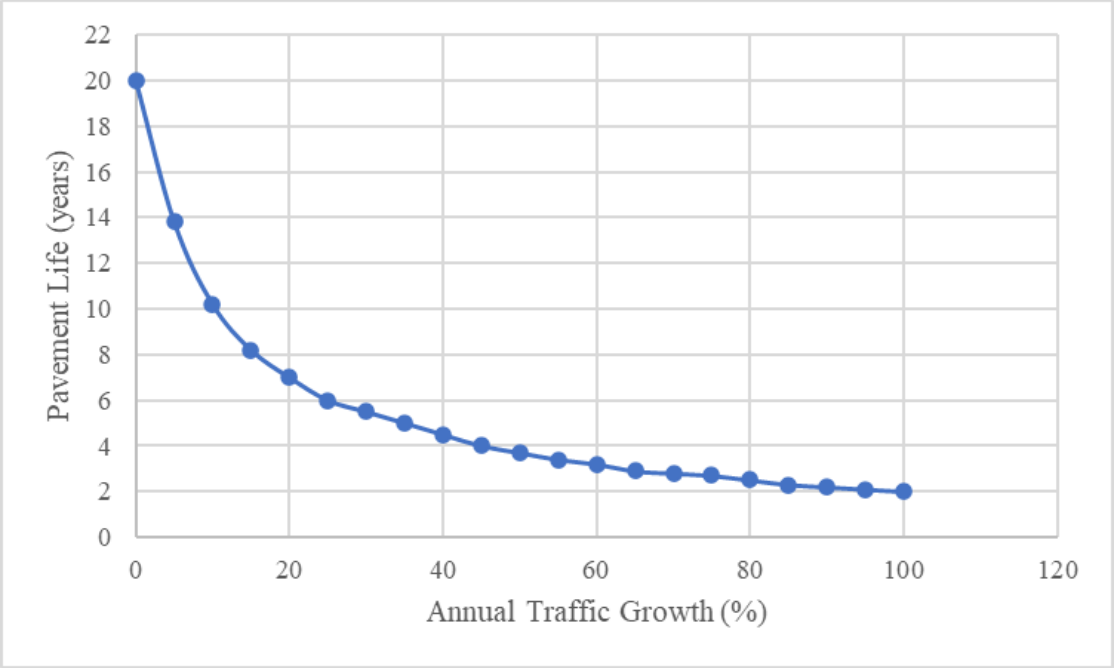

Figure 12. Effect of Traffic Growth on Projected Pavement Life.

The traffic category traffic mix is replaced by a user defined single wheel load that is equivalent to the calculated SWL of the critical aircraft in FAARFIELD. The annual departures of this vehicle are equivalent to the corresponding traffic category to simulate the repeated operations of the critical aircraft for the entire pavement life. Within FAARFIELD, Pavement Life Mode is selected and executed. The output is the estimated life of the pavement under the defined load, ignoring the effects of environmental fatigue. The user defined GVW for the SWL is then adjusted such that the estimated pavement life is 20 ($\pm$0.9) years, the full design life of the pavement. The GVW that results in a pavement life within the acceptable range is the load rating for repeated operations.

4.2.1.1. Load Rating for Repeated Operations Example

The Houston Southwest Airport (AXH) is used as an example. The airport experiences 42,588 annual operations, which places in the fourth GA airport traffic category. Collected GPR and FWD data indicate that the runway pavement structure consists of two inches of surface course over five inches of base and five inches of subbase over the subgrade, shown in Figure 13. Backcalculation using the MODULUS software produced the layer moduli values shown in Figure 14.

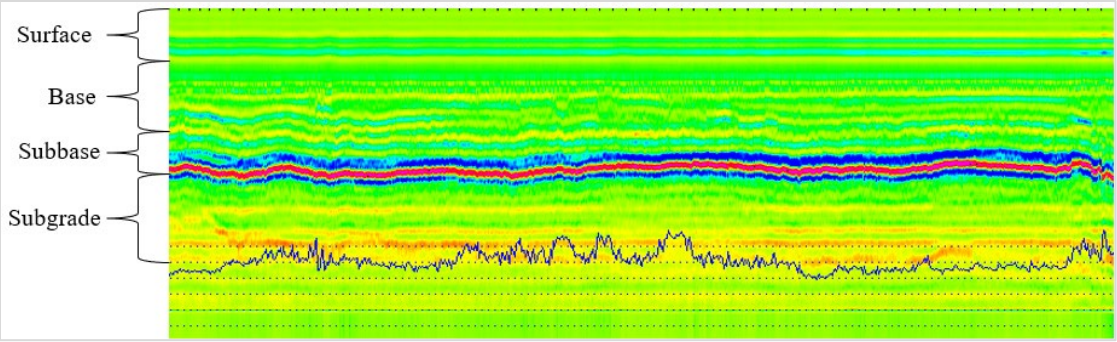

Figure 13. GPR Trace of Houston Southwest Airport (AXH) Runway.

Execution of the PCR analysis lists the Airbus A321neo as the critical aircraft with a maximum allowable GVW of 62,883 pounds. The resulting SWL is 31,442 pounds. Figure 15 displays the process of determining the load rating for repeated operations which resulted in a load rating of 28,900 pounds. Thus, for the pavement to withstand 20 years of traffic, aircraft operating out of Houston SW should not exceed 60,000 pounds.

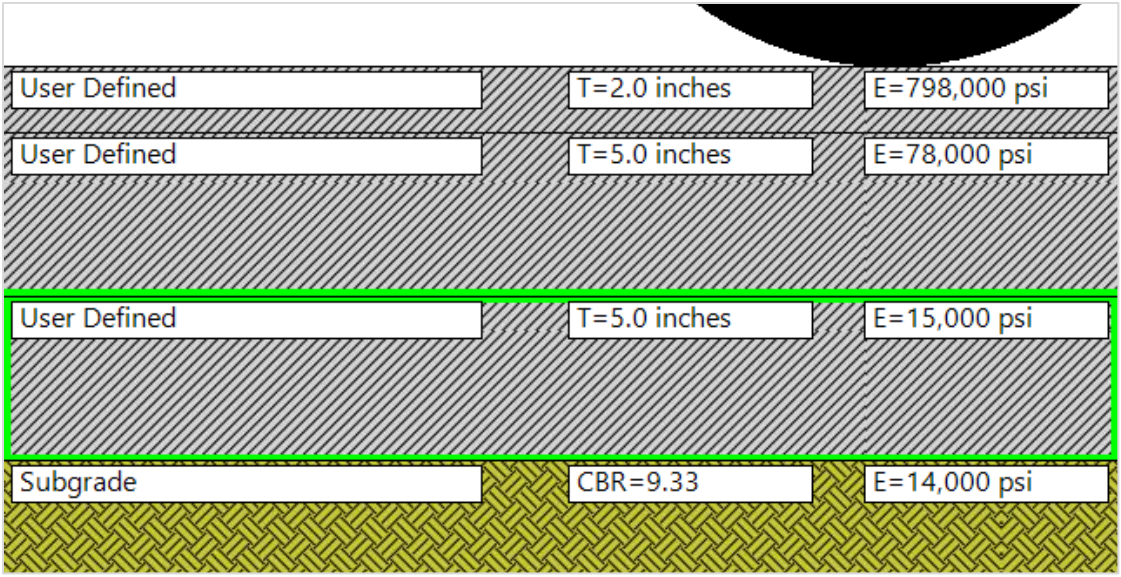

Figure 14. Houston SW Airport (AXH) Pavement Structure.

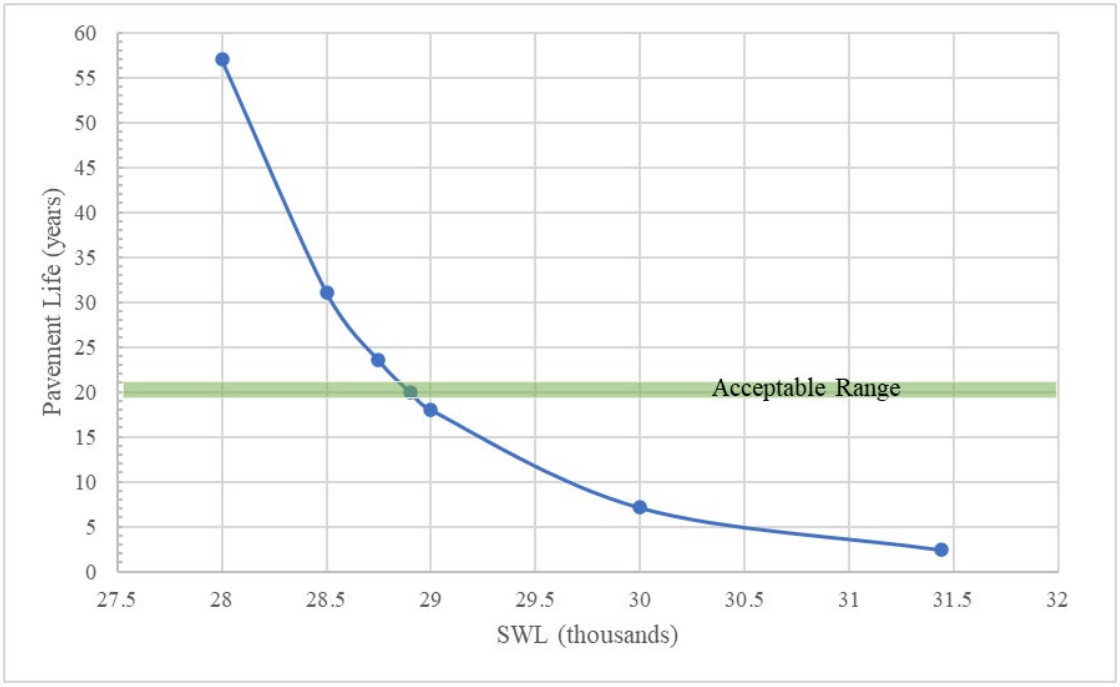

Figure 15. Load Rating for Repeated Operations at Houston SW Airport (AXH).

4.2.2. Single Use Load Rating

The procedure to load rate an airport pavement for a single operation is like the repeated operations procedure. The traffic category is selected based on the recorded annual traffic, and the layer moduli values are backcalculated. These inputs are entered into FAARFIELD, and the SWL rating is determined in the same manner as the repeated load rating. Once the SWL rating is determined, the SWL is entered as the sole vehicle in the traffic mix as before, but the annual departures category is set to one instead of the equivalent value for the traffic mix. The Pavement Life Analysis mode is then selected and executed. Figure 16 displays the required inputs and analysis specification for single use load rating. The result of the life analysis is the calculated pavement life to failure with a single annual departure. The user then adjusts the GVW of the SWL and executes the life analysis until the output is greater than or equal to one year, but less than two years. The GVW at this iteration is the maximum load the pavement can sustain for one operation and is recorded as the single use load rating.

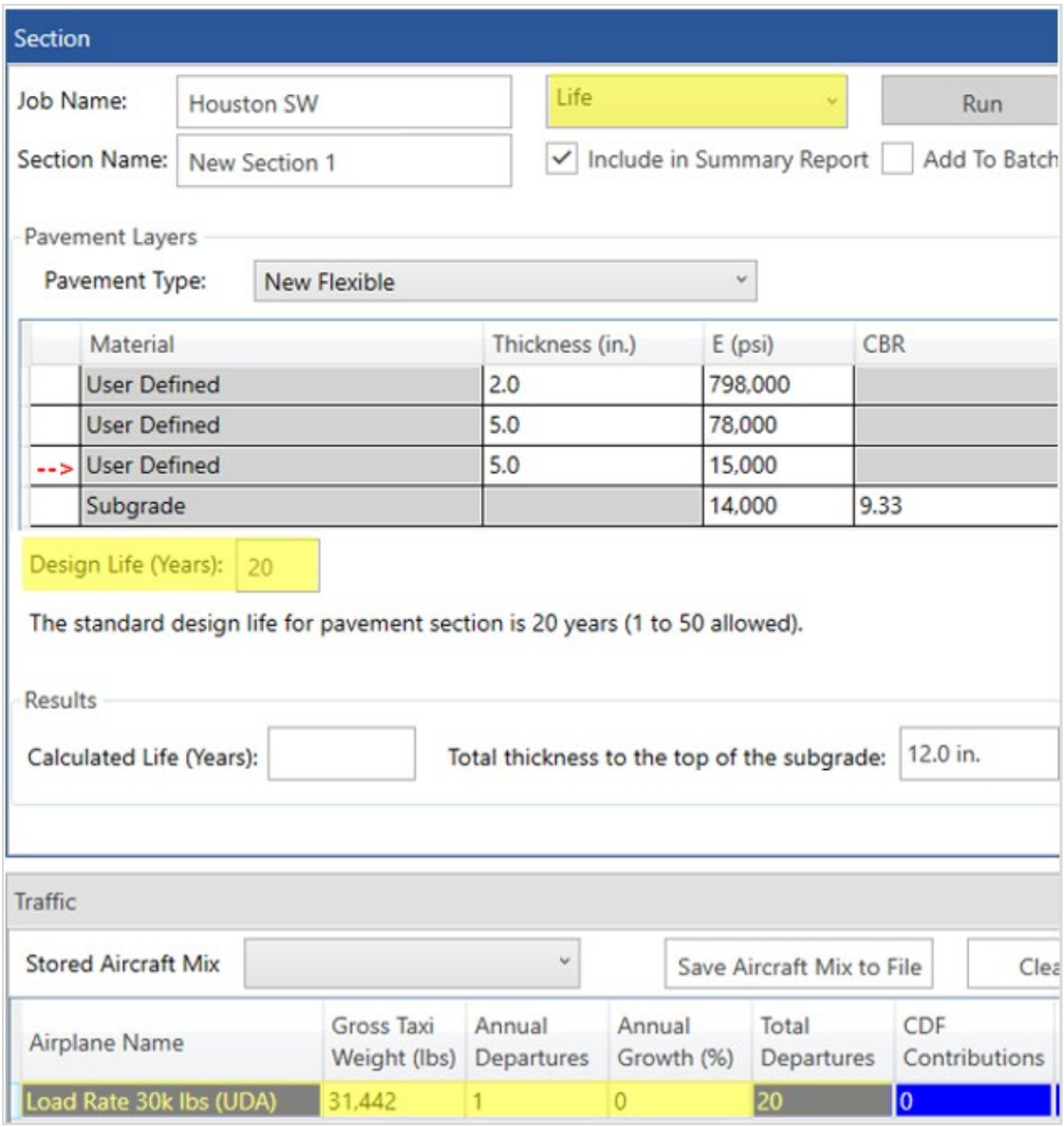

Figure 16. Required Specifications for Single Use Load Rating for Houston SW Airport (AXH) (Annotated).

4.2.2.1. Single Use Load Rating Example

The Houston SW Airport will again be used as an example for the single use load rating procedure. The same structure and layer moduli values are used as shown in Figure 14, and the

airport falls within the fourth airport traffic category with over 40,000 annual traffic operations. The calculated SWL rating is 31,442 pounds, which is greater than the SWL calculated from the repeated load rating process. The results of the life analysis iteration are displayed in Figure 17. It is determined from the simulation that a 225,000 pound SWL results in an expected pavement life of one year, thus 225,000 pounds is the single use load rating for this pavement. This value should not be used to determine regular traffic capacity but should be utilized in emergency situations to allow for large military and emergency aircraft to safely operate out of this facility on a single occasion.

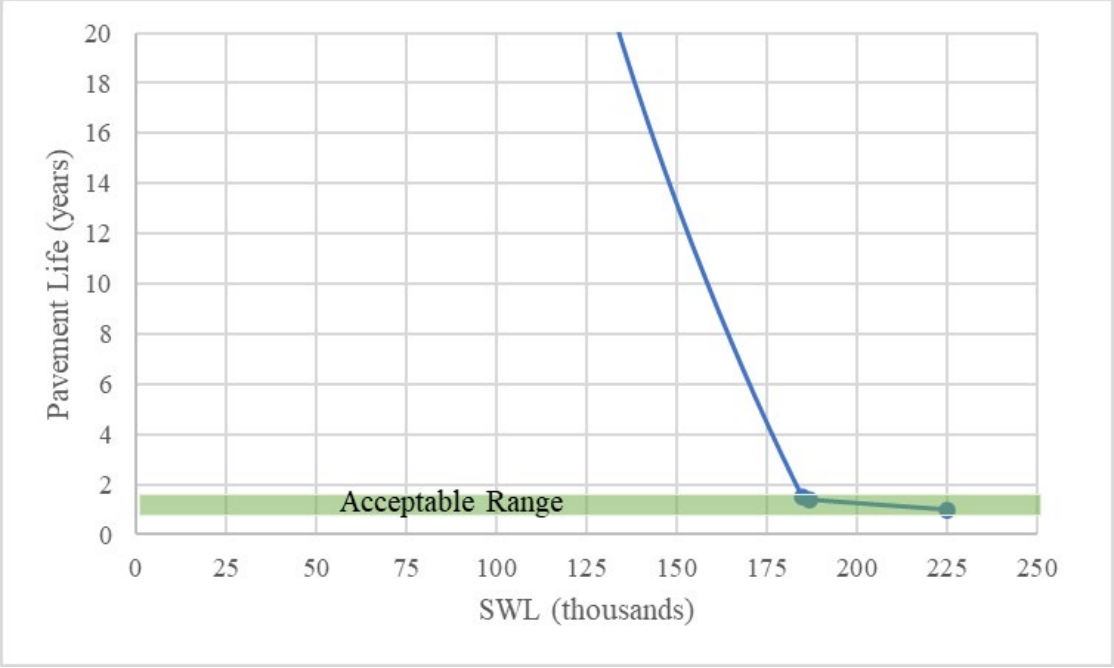

Figure 17. Single Use Load Rating at Houston SW Airport (AXH).

5. LOAD RATING RESULTS

The following sections (5.1-5.2) discuss the results of the NDT conducted at each airport and the load rating results generated by FAARFIELD using the gathered data. The testing plan outlined in Table 9 was utilized to standardize the data collection. GPR and FWD data were collected for the aprons, taxiways, and runways at each airport as shown in Figure 18.

Table 9. GA Airport NDT Testing Plan.

Data	Procedure
FWD	• First drop 100 ft. away from the runway end with the lower number. • Subsequent drops at every 100 ft. • Runways between 50-75 ft. wide will require two passes: one run 8 ft. left of the center stripe and another 8 ft. right of the center stripe. • Runways greater than 75 ft. in width will require four passes: 8 ft. and 16 ft. left of the center stripe, and 8 ft. and 16 ft. right of the center stripe. • Each run should be collected from the lower end of the runway to the higher end. • Collect on all runways unless otherwise noted. • Additional drops should be done on the primary taxiway near the hold short lines when possible, the fueling area, and the main parking area. • The location of additional drops to be marked with an X on the layout map. • Collect FWD on the taxiways using the same orientation as the runway collection.
GPR	• Runways between 50-75 ft. wide will require two passes: one run 8 ft. left of the center stripe and another 8 ft. right of the center stripe. • Runways greater than 75 ft. in width will require four passes: 8 ft. and 16 ft. left of the center stripe, and 8 ft. and 16 ft. right of the center stripe. • Each run should be collected from the lower end of the runway to the higher end. • Only one run is necessary per additional location highlighted on the layout map. • Additional runs should be done down the center of the taxiway, starting and stopping at the hold short lines using the same orientation as the runway collection. • Additional collection should be completed in one run when possible.

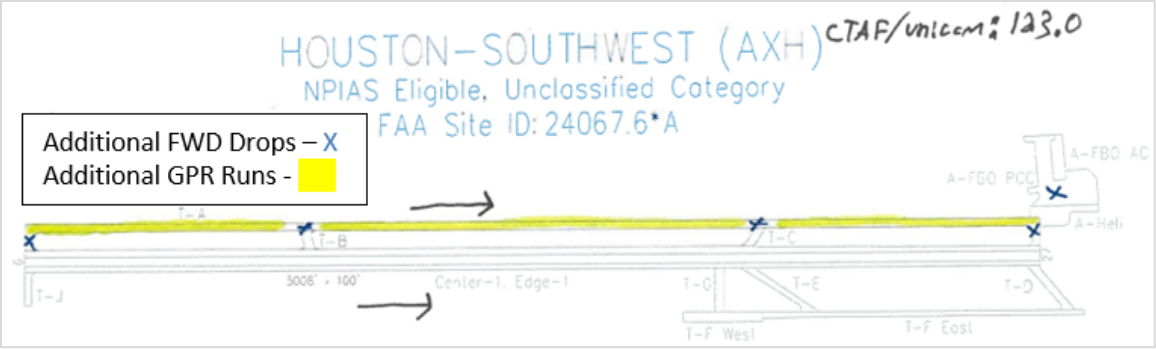

Figure 18. NDT Airport Testing Plan for Houston SW Airport (AXH).

5.1. Non-Destructive Testing

GPR data indicated that the pavement structure of eight of the ten tested airport runways consists of four material layers: a flexible surface course and a base and subbase layer over the natural subgrade. Two of the tested airports did not have a subbase course but consisted of a two-layer pavement structure over the subgrade material. In some instances, GPR data were used to identify points of structural weakness due to subsurface moisture or structural irregularities. Figure 19 displays the measured layer thicknesses determined by the GPR. These values were used in conjunction with deflection data shown in Figure 20 to backcalculate layer moduli values in Figure 21.

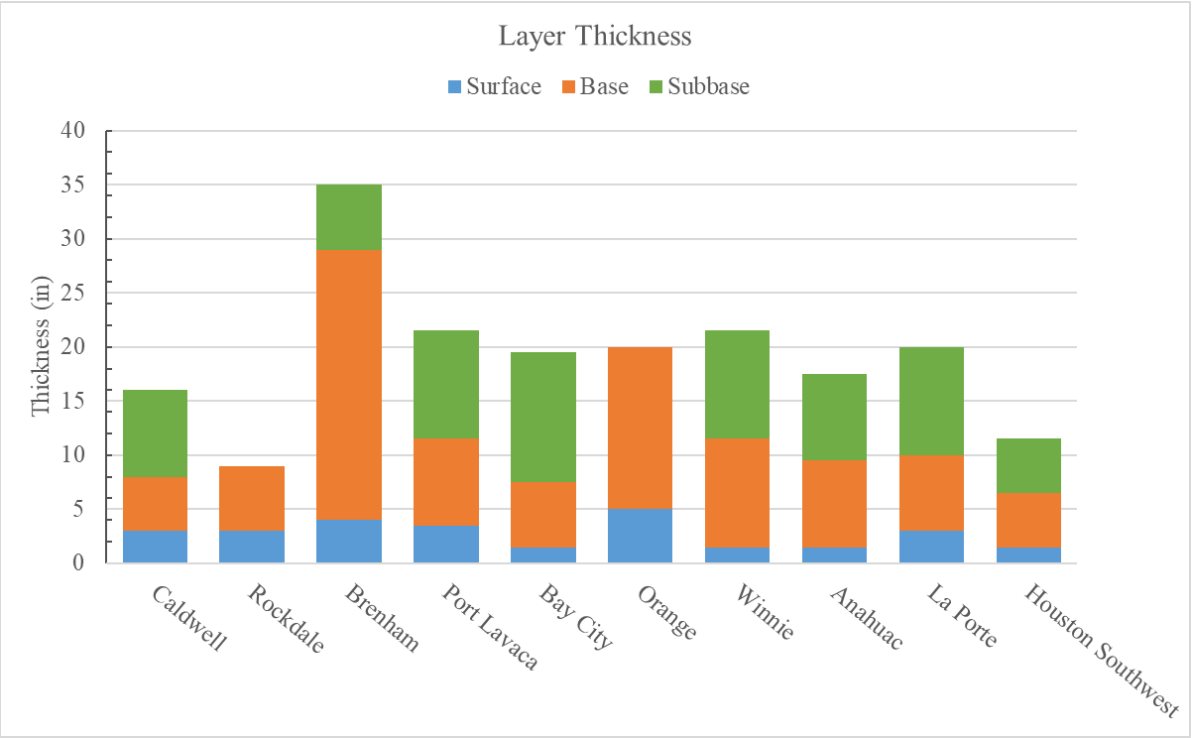

Figure 19. Tested Runway Layer Thickness.

On roadway infrastructure, the expected deflection values measured by the FWD are on the scale of ten mils or less. Deflection readings greater than ten mils are often signs of structural failure. However, this was not the case for the tested airport pavements. Figure 20 is a box and whisker plot indicating that the threshold signifying structural failure of an airport runway is greater than ten mils. In general, it was found that normal deflections for the tested GA airports were 20-40 mils.

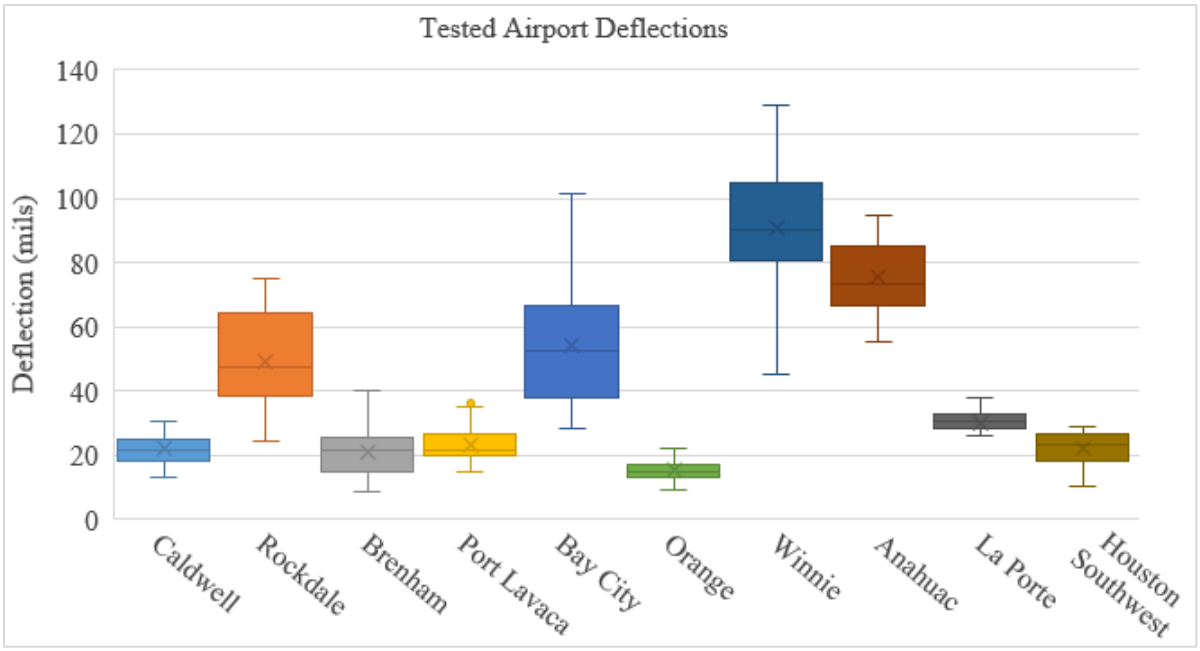

Figure 20. Maximum Deflection Values for Tested Airports.

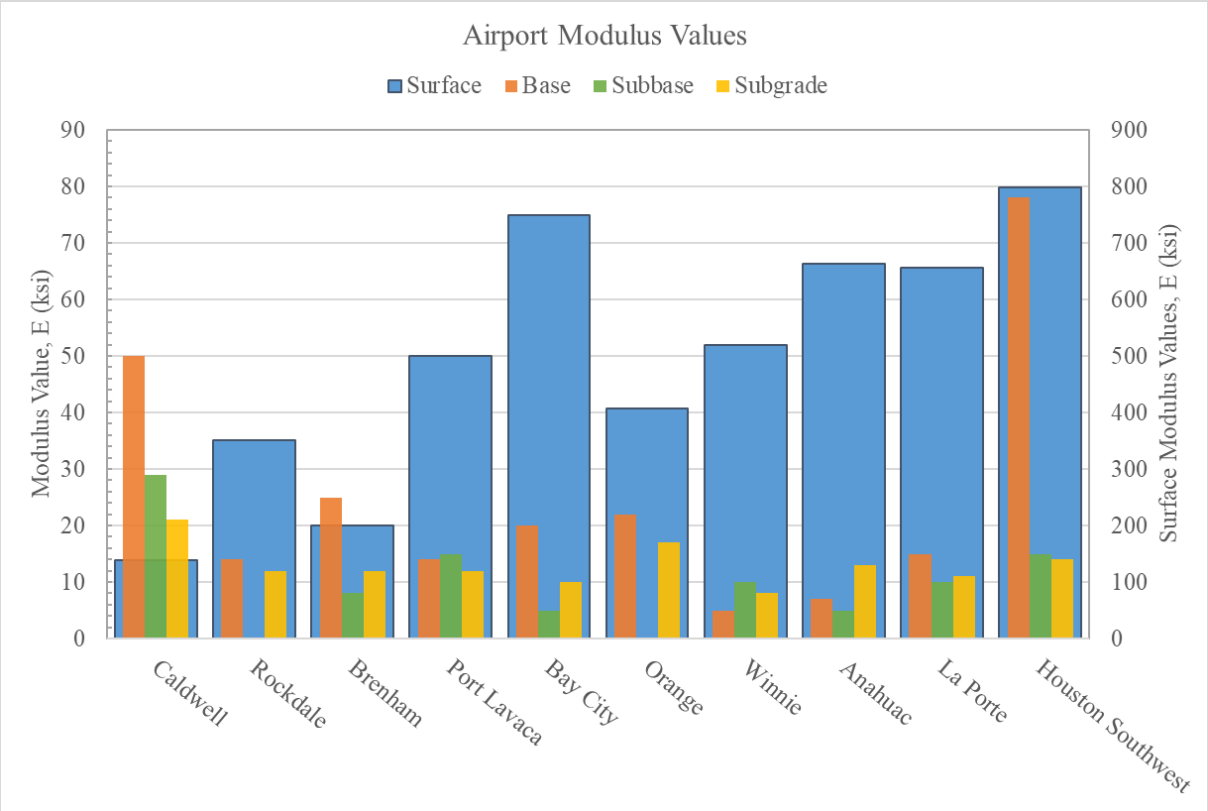

Figure 21. Airport Backcalculated Layer Moduli Values.

The calculated base values were found to be weak on many of the airports, so the modulus calculations were compared to the base curvature index (BCI) of the runways, calculated as the difference between the FWD sensors 12 (D12) and 24 (D24) inches away from the load center as shown in Equation 12 [51]:

$$\boldsymbol{BCI = D12 - D24} \tag{12}$$

BCI values are rated by TxDOT using Table 10. The pavement surface courses range from 2-5 inches thick, therefore the BCI values were evaluated based on the criteria listed for surface thickness from 2.5-5 inches. The resulting BCI ratings agree with the backcalculated

base moduli values. The base layers of half the tested airports are considered poor or very poor condition as shown in Figure 22. While such weak base courses are unexpected, the life a performance of the runways is not compromised. Equivalent base layers on a roadway would be insufficient due to the volume of traffic and associated loads, but the traffic experienced by the tested GA airports is markedly less. What would be structural failure on a road does not greatly impact the runway service.

Table 10. BCI Classification System.

Surface Thickness (in.)		**5**	**5-2.5**	**2.5-0.5**	**0.5**
BCI Rating	Very Good	< 2	< 3	< 4	< 8
	Good	2-3	3-5	4-8	8-12
	Medium	3-4	5-9	8-12	12-16
	Poor	4-5	8-10	12-16	16-20
	Very Poor	> 5	> 10	> 16	> 20

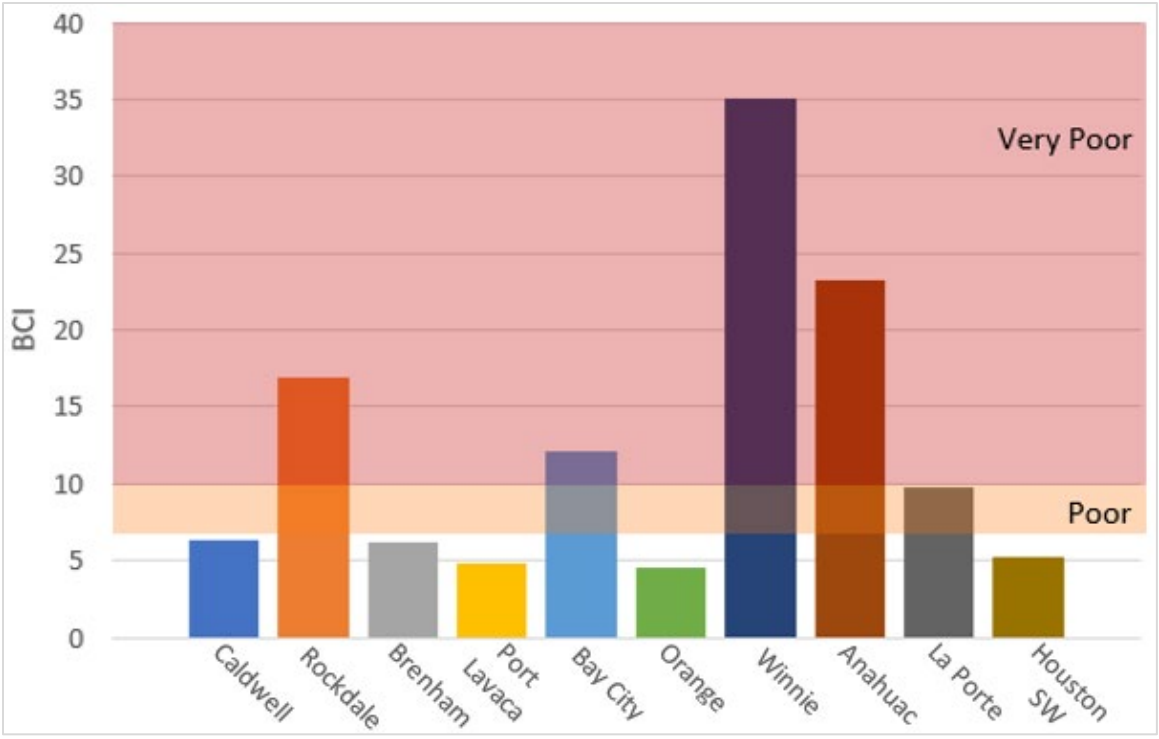

Figure 22. Average BCI Values and Corresponding Ratings.

5.2. FAARFIELD Results

The load rating results produced by FAARFIELD are consistent with the expected outputs, given the actual traffic expectations and pavement structures and characteristics determined from NDT. However, the SWL rating is more controlled by the pavement structure and layer strengths than the traffic. Figure 23 displays the SWL calculated from the traffic mix within the FAARFIELD PCR report. The airports with the top three greatest SWL ratings are Orange, Caldwell, and Port Lavaca. Each of these airports are in the second traffic category and have medium to good BCI ratings. Houston Southwest airport is the only airport included within the fourth traffic category yet ranks in the three lowest SWLs.

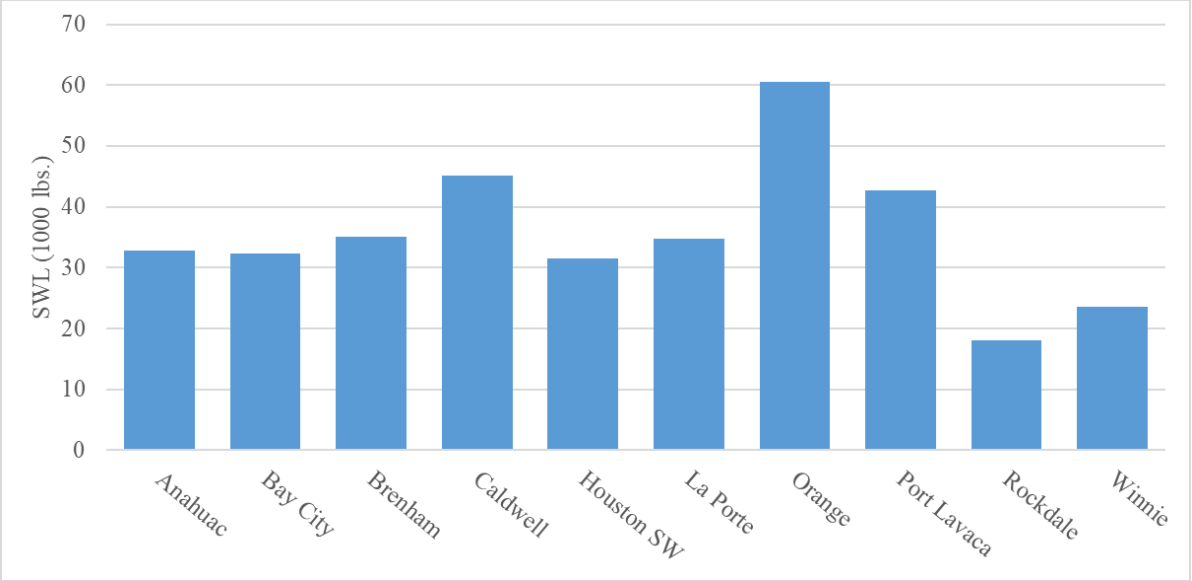

Figure 23. Tested Airport SWL from Traffic Mix.

To ensure repeatable SWL results, the SWL calculated from the critical aircraft of the traffic mix is compared to the SWL rating for repeated operations in Figure 24. Following the load rating procedure described in Section 4, the SWL calculated from the traffic mix is adjusted until the service life of the pavement is 20 years, where the resulting SWL is the rating for repeated operations. The difference in SWL values was at most 20 percent for all airports except Orange and Port Lavaca in which the difference was 36 and 23 percent, respectively, indicating that the FAARFIELD load ratings are repeatable.

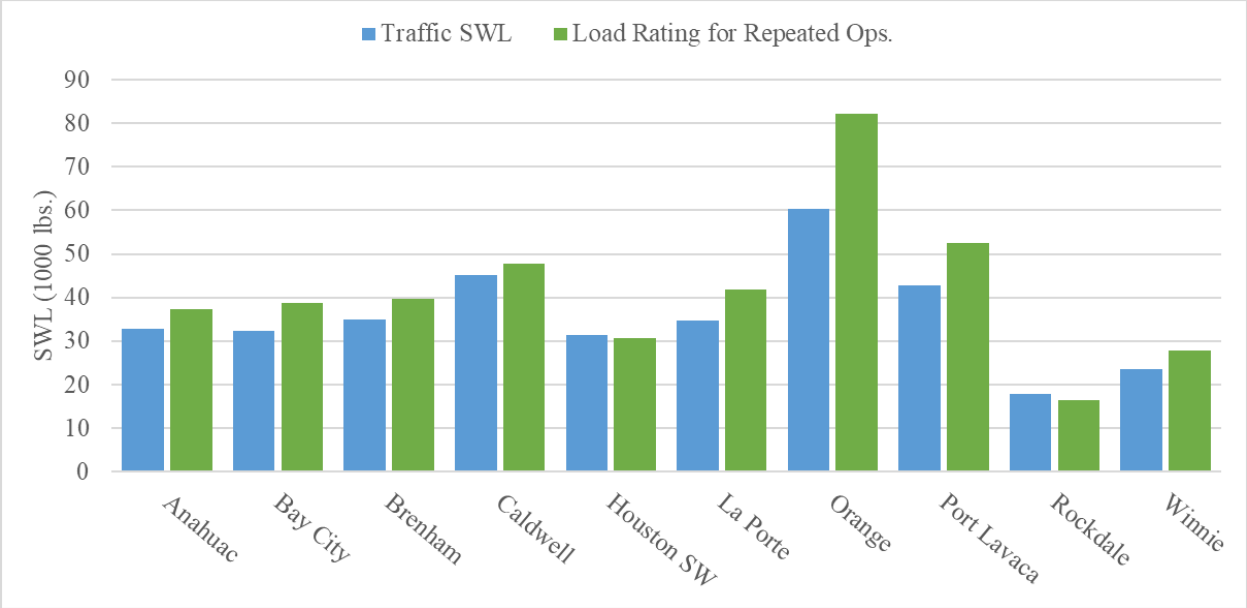

Figure 24. Comparison of SWL Computed from the Critical Aircraft and SWL rating for Repeated Operations.

Figure 25 compares the SWL for repeated operations to the single use SWL rating. On average, the single use SWL was four to five times greater than the SWL for repeated operations. This indicates that it is expected a GA airport is capable of sustaining an aircraft that has a SWL four to five times greater than the SWL rating for repeated operations for a single emergency operation.

Figure 25. Comparison of SWL Rating for Repeated Operations and Single Use.

6. FLOOD EVENT SIMULATION

To better understand the capabilities of GA airports during climate emergencies, FAARFIELD was used to simulate the pavement response when the subsurface layers are inundated with water. Literature indicates that the modulus of elasticity experiences a 25 percent reduction when the material is saturated [16]. This condition was applied to the airport runway structures within FAARFIELD, and the single use load rating was determined at each phase of the simulation as a measurement of the pavement structural capacity. Figure 26 provides an outline of the flood simulation.

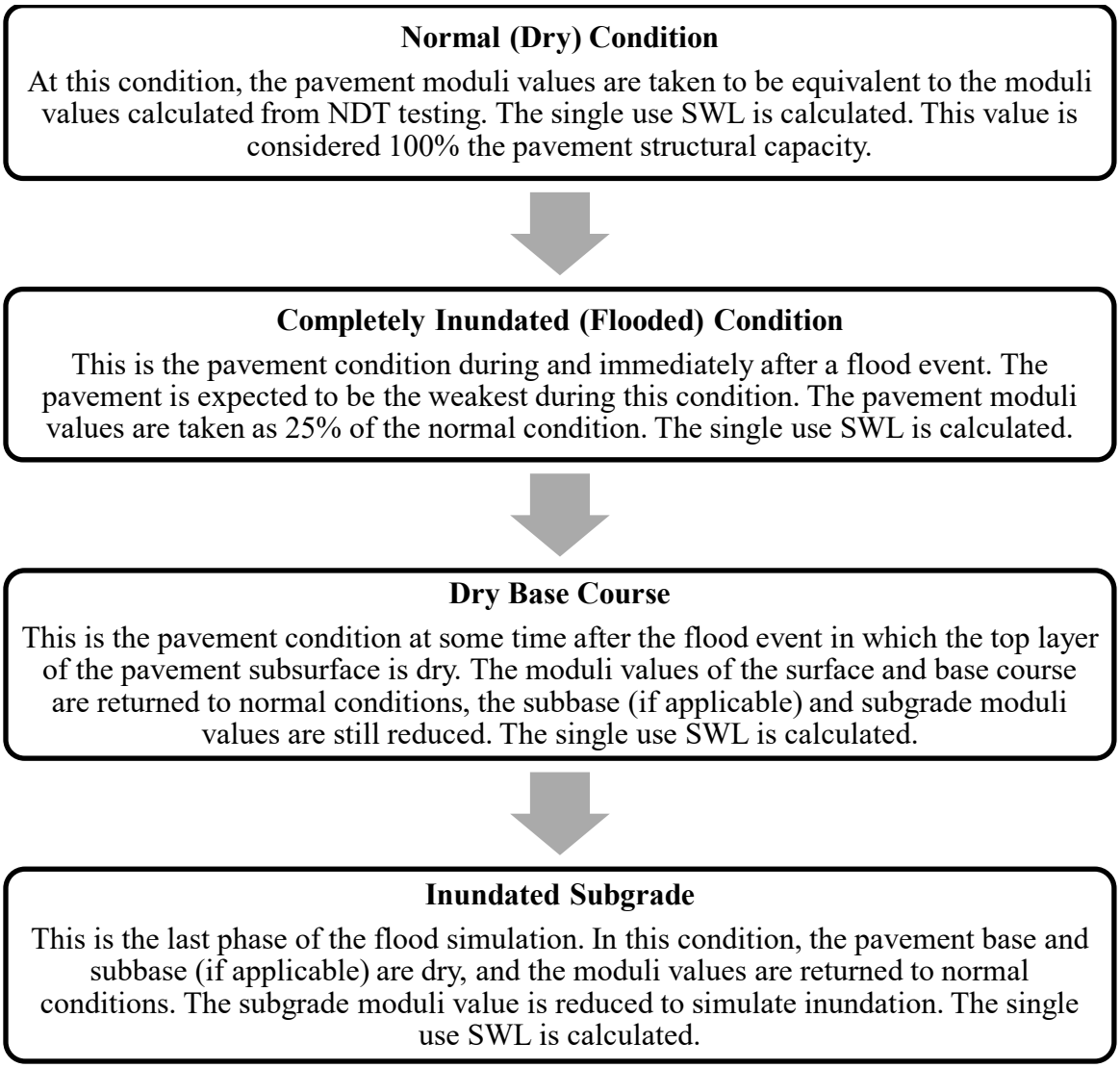

Figure 26. Flood Event Simulation Process.

6.1. Flood Event Results

Figure 27 presents the results of the flood simulation for each airport runway. The Orange airport maintained the highest single use SWL rating throughout the simulated flood event. This is as expected, as NDT results show that Orange has the lowest BCI value,

suggesting that the base at this airport is stronger than the base courses at other tested airports. On average, airports experienced a 24% reduction in SWL capacity during the complete inundation condition. This matches well with the 25% reduction in layer moduli values during saturated conditions.

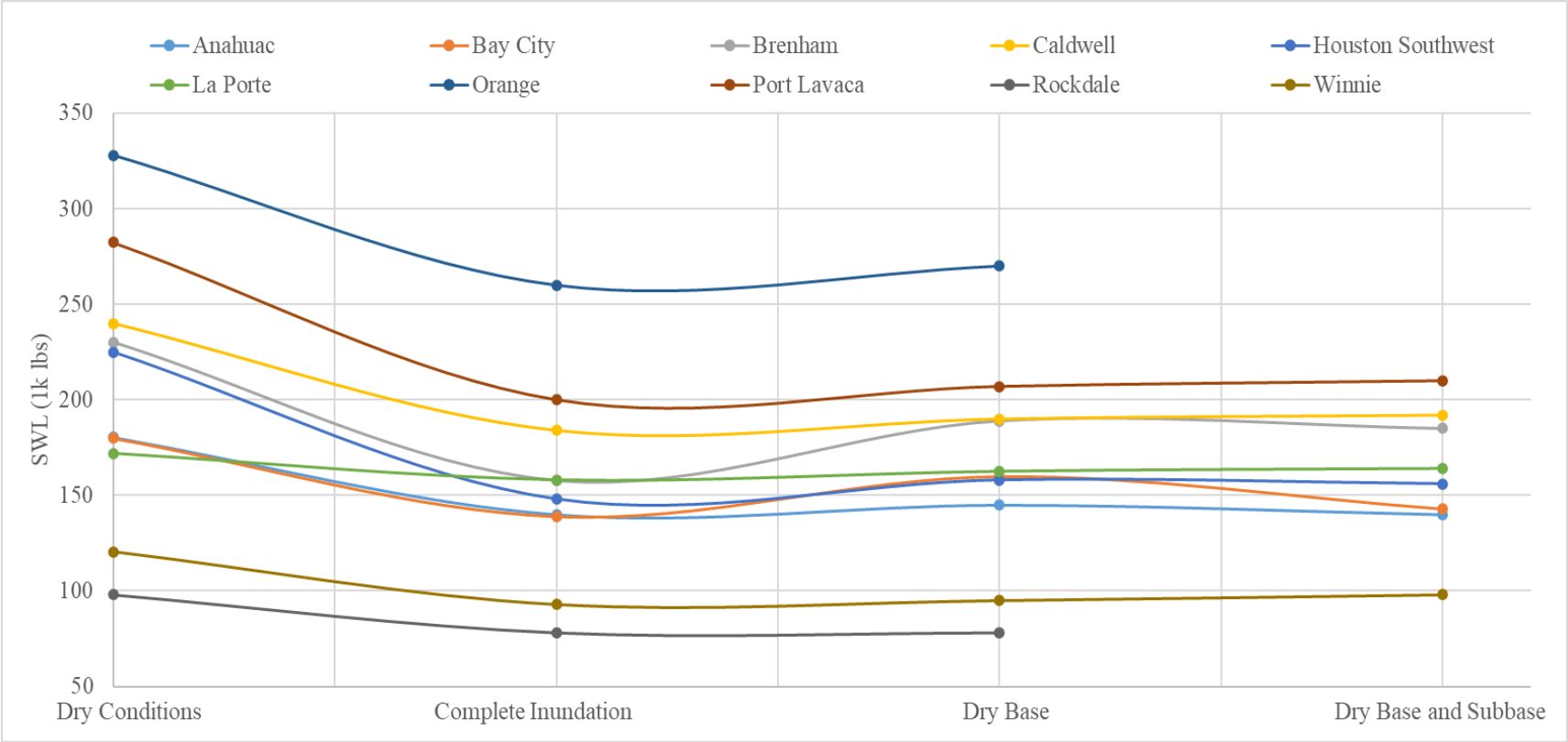

Figure 27. Flood Simulation Results.

The expected results of the flood event simulation were that the pavement base layers would control the pavement loading capacity. This was expected because literature suggests that the greatest increase in structural capacity occurs at the interface of the base/subbase and subgrade. However, the data presented in Figure 28 shows that the structural capacity for these airports is controlled by the pavement subgrade, as the subgrade layer, when inundated, reduces the structural capacity of the pavement more than the base/subbase layers. This outcome may be due to the weak base courses at most of the tested airports. The table in Appendix B numerically displays the single use SWL and reduction in capacity for each phase of the simulation.

Another unexpected outcome from the simulation was four of the ten airports tested experienced a decrease in load capacity at the last phase of the simulation, in which all subsurface layer moduli are returned to normal except the subgrade, which is reduced by 25 percent. These airports, shown in Figure 29, each have four layered pavement structures of varying thicknesses and categorized in different traffic categories. However, the average reduction in capacity was less than or equal to 2 percent for each airport except Bay City, which experienced a 10 percent reduction at this stage.

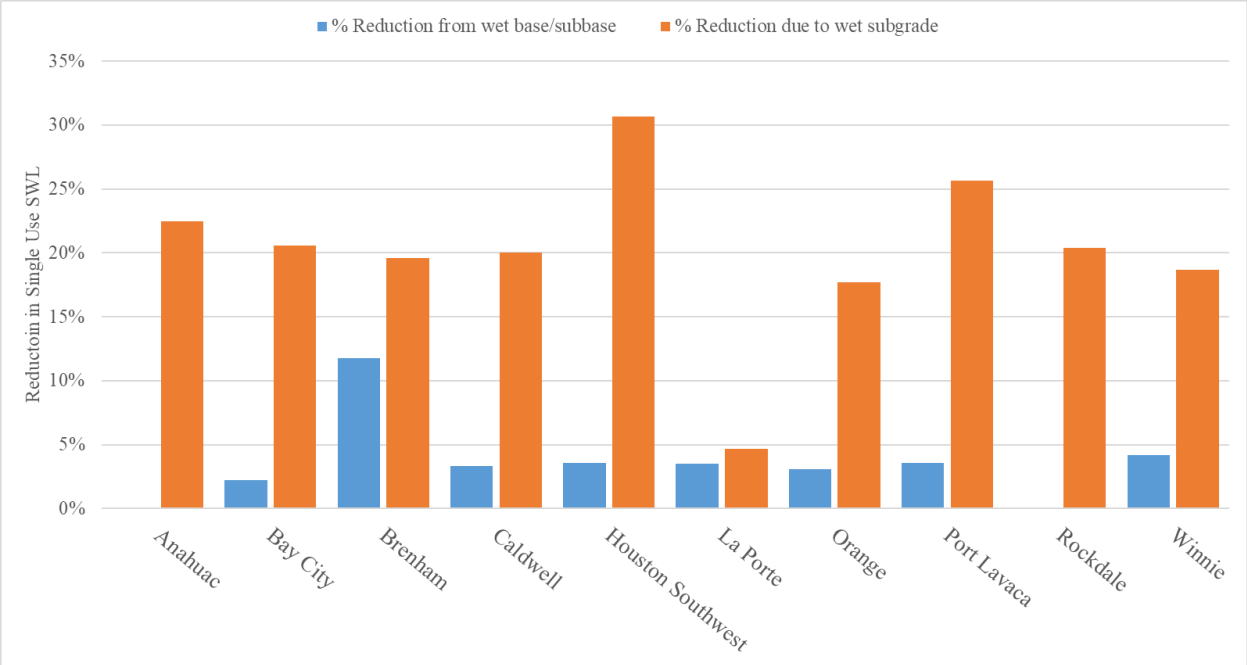

Figure 28. Percent Strength Reduction for the Base/Subbase Compared to the Subgrade Layers During Flood Event.

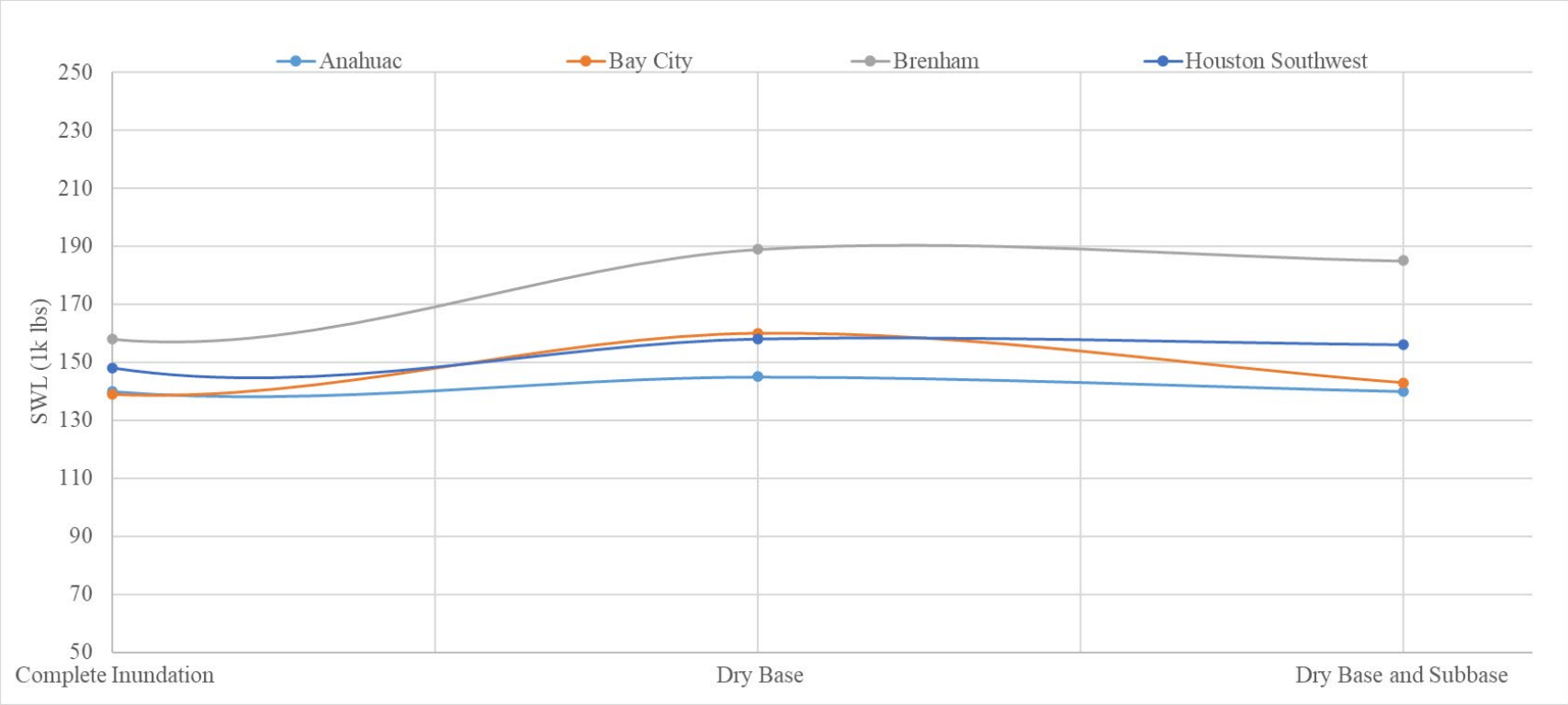

Figure 29. Single Use SWL During and After Flood Event.

6.2. Pavement Structural Recovery

In addition to characterizing runway structural capabilities during flood events, there is a need to determine the relative time period in which the pavement will regain strength after the event. Saturated hydraulic conductivity (Ksat) is a physical property of a soil that quantifies the ability of a saturated soil to transmit water across a hydraulic gradient. The flow rate of water through the saturated soil is calculated using Darcy's law, shown in Equation 13 [52]. The United States Department of Agriculture (USDA) utilizes the saturated hydraulic conductivity value in categorizing regions into natural drainage classes listed in Table 11. Additionally, the saturated hydraulic conductivity value alone is classified in Table 12. In general, soils having low conductivity values have high clay content, while soils with high conductivity values are sandy and therefore more conducive to the flow of moisture [52].

$$\frac{Q}{At} = -K_{sat}\frac{dH}{dz} \tag{13}$$

Where

Q/At = flow rate of water

K_{sat} = saturated hydraulic conductivity

dH/dz = hydraulic gradient

Table 11. USDA Natural Drainage Classes.

Class	Description
Excessively Drained	Soils have a very high Ksat value. Water is promptly removed.
Somewhat Excessively Drained	Soils have high Ksat values and are typically coarse textured. Internal water is very rare.
Well Drained	Water retention is conducive to plant growth. Internal water may occur deep beneath the surface.
Moderately Well Drained	Soils have a lower Ksat value. Water is removed slowly during parts of the year.
Somewhat Poorly Drained	Soils have low Ksat values. Internal water near the surface is common.
Poorly Drained	Soils have a very low Ksat value. Shallow depths remain wet for extended periods of time, and free water may be at the surface.
Very Poorly Drained	Water remains at or near the surface for much of the year, and ponding is frequent.
Subaqueous	Internal water is permanent. Water is above the surface of the soil.

Table 12. Ksat Classes.

Class	Ksat (in/hr)
Very Low	0.000 to 0.001
Low	0.001 to 0.015
Moderately Low	0.015 to 0.15
Moderately High	0.15 to 1.5
High	1.5 to 15
Very High	15 to 100

Application of the saturated hydraulic conductivity property and Darcy's Law to GA airports requires geotechnical knowledge of the natural subgrade. For the purpose of this

research, the subgrade is the only material analyzed and classified using saturated hydraulic conductivity, as it was determined by the flood simulation that the subgrade contributes most to the structural capacity of the airfield pavement. The USDA's Web Soil Survey website is used in this work to conduct a geotechnical survey of the material between 12 and 24 inches beneath the surface at each of the tested airports. Using the interactive map, the airport is located and bound within the area of interest as shown in Figure 30, where the subgrade material boundaries are shown in orange. This allows the user to select data from the USDA's geotechnical report on the area. The geotechnical information, including the AASHTO group classification of the predominate soil, plasticity index (PI), and saturated hydraulic conductivity value for the tested airports is shown in Appendix C.

Figure 30. Winnie/Stowell Airport (T90) Soil Map within Web Soil Survey. Reprinted from [53]**.**

The results of the geotechnical survey indicate that the saturated hydraulic conductivity values of all the tested airports except Rockdale are classified as either low or moderately low. These classifications would suggest that, in the event the subsurface materials become inundated, the pavement structure would need a substantial period of time before the structural capacity is restored. However, Figure 31 compares the conductivity classification to the drainage class for each airport. The data suggests the drainage class is not reliant upon the saturated hydraulic conductivity value. Even if the conductivity value is poor, flooding may be mitigated if the drainage is substantial. For example, the hydraulic conductivity value alone implies that the Houston Southwest and La Porte airports are at the greatest risk of flooding, but wholistic data indicates the Orange and Winnie airports are at greater risk of major flooding than the other airports because both the drainage and saturated hydraulic conductivity classes are low.

Figure 31. Comparison of Airport Ksat and Drainage Classifications.

The saturated hydraulic conductivity value and drainage class of the airport subgrade is beneficial for understanding the effects climate events may have on the airport pavement. However, use of the saturated hydraulic conductivity soil property and hydraulic gradient may not be best practice to determine the structural capacity of a drying pavement in an emergency situation. Because the saturated hydraulic conductivity value is only applicable for fully saturated pavements, subsurface moisture conditions may still be greater than optimum. To best determine which pavement layers are inundated, a monitoring well may be installed to monitor the height of the water table. In this manner, operators will know precisely which subsurface materials are inundated such that a load rating procedure may be executed with engineering judgement.

7. CONCLUSIONS

The purpose of this research was to develop a methodology to load rate GA airports with consideration for environmental conditions, specifically a flood event. Historical data containing traffic volumes for use in the load rating processes were not available for the airports tested, so the research developed a method to categorize GA airports based on designed traffic mixes. The traffic mixes were designed to represent accurate traffic data for each GA airport, including popular aircraft models and realistic annual operation totals. Table 13 summarizes this work and displays the load rating figures associated with each airport. The study was successful in utilizing available FAA software and tools to load rate airport pavements for repeated operations and single use. The research also utilized these tools to determine the effects of subsurface water inundation on the pavement load capacity. The following conclusions were drawn from the results of the research:

- The measured airport pavement deflections are much higher than expected roadway values.
- The majority of tested airports have structurally weak base layers, but pavement life and performance are not adversely affected due to low volumes of traffic compared with typically highway type loading.
- FAARFIELD can produce accurate and repeatable SWL ratings for both repeated operations and single use.
- Single use SWL ratings are, on average, about 5 times the SWL rating for repeated operations. However, the airport pavement is expected to fail under the loads of an aircraft that is equivalent to the single use SWL. Therefore, it is strongly recommended

that the pavement surface be inspected after landing to ensure a takeoff operation is possible.

- The inundation of the subgrade layer had a greater effect on the structural capacity of the runway than the base layer.
- Literature indicates that pavement subsurface inundation produces non-recoverable damages to structural capabilities and will result in loss of pavement life.
- The saturated hydraulic conductivity property and hydraulic gradient are not recommended to predict subsurface moisture in emergency situations. The most accurate determination of subsurface inundation is through water table measurements procured by a monitoring well.

Table 13. Summary of Completed Work.

Airport Name	Annual Traffic	GA Traffic Category	SWL for Repeated Operations	Single Use SWL Rating
Anahuac	2,392	1	37,300	180,500
Bay City	14,196	2	38,715	180,000
Brenham	27,664	3	39,660	230,000
Caldwell	7,072	2	47,700	240,000
Houston Southwest	42,588	4	30,650	225,000
La Porte	29,120	3	41,805	172,000
Orange	12,376	2	82,280	299,100
Port Lavaca	8,736	2	52,480	161,800
Rockdale	3,588	1	16,370	67,950
Winnie	5,980	2	27,825	120,000

7.1. Future Work

Future work on this topic largely involves study on new FAA standards for ACR/PCR determination, and use of FAARFIELD. A determination of the relationship between PCR and pavement strength was not concluded in this study, as PCR values varied depending on the critical aircraft within a given traffic mix. Airports may opt to publish annual PCR ratings with load rating values. Additional work is also needed to refine the load rating process. FAARFIELD is a pavement design program. As such, there is currently no method to input existing distresses, whether surface or structural, and pavement life values produced by FAARFIELD may be optimistic when compared to methods more commonly used to estimate roadway pavement life. Lastly, this study recommends conducting a geotechnical survey to better understand the material properties of the natural subgrade. Connections may be found between the physical soil properties and the moisture effects on strength discussed in this research.

REFERENCES

[1] Federal Aviation Administration, "General Aviation Airports: A National Asset," Federal Aviation Administration, Washington, DC, 2012.

[2] Texas Department of Transportation, "Texas Airport Directory Map," March 2016. [Online]. Available: https://maps.dot.state.tx.us/TADSMap/.

[3] R. M. Sorenson, Basic Coastal Engineering Thrid Edition, New York: Springer, 2006.

[4] Civil Air Patrol, "CAP.News," Global Reach, 2022. [Online]. Available: https://www.cap.news/cap-aircrew-links-300-stranded-by-harvey-flooding-to-needed-help/. [Accessed 10 2 2023].

[5] D. Walker, L. Entine and S. Kummer, PASER - Pavement Surface Evaluation and Rating Asphalt Airfield Pavements, University of Wisconsin-Madison, 2014.

[6] Federal Aviation Administration, *Advisory Circular: Development of State Aviation Standards for Airport Pavement Construction,* Federal Aviation Administration, 2019.

[7] J. Sun, G. Chai, E. Oh and P. Bell, "A Review of PCN Determination of Airport Pavements Using FWD/HWD Test," *Int. J. Pavement Res. Tecnol.,* 2022.

[8] C. FABRE, *The Aircraft Classification Rating-Pavemtent Classification Rating ACR-PCR,* Quito: ICAO, 2018.

[9] Austrailian Government Civil Aviation Safety Authority, "Advisory Circular: Strength Rating of Aerodome Pavements," Civil Aviation Safety Authority, 2021.

[10] Federal Aviation Administration, "Advisory Circular: Standardized Method of Reporting Airport Pavement Strength - PCR," Federal Aviation Administration, Draft.

[11] M. H. Elshaer, "Assessing the Mechanical Response of Pavements During and After Flooding," 2017. [Online]. Available: https://scholars.unh.edu/dissertation/160.

[12] M. S. N. Ismail, A. N. A. Ghani, Z. M. Ghazaly and M. Dafalla, "A Study on the Effect of Flooding Depths and Duration on Soil Subgrade Performance and Stability," *Int. J. of GEOMATE,* vol. 19, no. 71, pp. 182-187, July 2020.

[13] Z. Zhang, Z. Wu, M. Martinez and K. Gaspard, "Pavement Structures Damage Caused by Hurricane Katrina Flooding," *Journal of Geotechnical and Geoenvironmental Engineering,* vol. 134, no. 5, 2008.

[14] P. Vennapusa, D. White and K. Miller, "Western Iowa Missouri River Flooding - Geo-Infrastructure Damage Assessment, Repair and Mitigation Strategies," Center for Earthworks Engineering Research, Ames, IA, 2013.

[15] "Asset Management, Extreme Weather, and Proxy Indicators Pilot Final Report," Texas Department of Transportation, 2019.

[16] M. G. M. Elshaer and J. S. Daniel, "Impact of Subsurface Water on Structural Performance of Inundated Flexible Pavements," *International Journal of Pavement Engineering,* vol. 20, no. 8, pp. 947-957, 2019.

[17] X. Chen and Z. Zhang, "Effects of Hurricanes Katrina and Rita Flooding on Louisiana Pavement Performance," ASCE, 2014.

[18] S. M. Hossain and W. S. Kim, "Estimation of Subgrade Resilient Modulus Using the Unconfined Compression Test," National Technical Information Service, Springfield, VA, 2014.

[19] E. V. Edris, *Dynamic Properties of Subgrade Soils, Including Environmental Effects,* Texas A&M University, 1976.

[20] K. Naji, "Resilient Modulus-Moisture Content Relationships for Pavement Engineering Applications," *International Journal of Pavement Engineering,* vol. 19, no. 7, pp. 651-660, 2018.

[21] A. N. A. Ghani, N. I. Roslan and A. H. A. Hamid, "Road Submergence During Flooding and its Effect on Subgrade Strength," *International Journal of GEOMATE,* vol. 10, no. 21, pp. 1848-1853, 2016.

[22] Y. Y. Perera, C. E. Zapata, W. N. Houston and S. L. Houston, "Long-Term Moisture Conditions Under Highway Pavements," *Geotechnical Engineering for Transportation Projects,* 2004.

[23] S. Hu, F. Zhou and T. Scullion, "Development of Texas Mechanistic-Empirical Flexible Pavement Design System (TxME)," National Technical Information Service, Alexandria, VA, 2013.

[24] E. C. Drumm, J. S. Reeves, M. R. Madgett and T. D. William, "Subgrade Resilient Modulus Correction for Saturation Effects," *Journal of Geotechnical and Geoenvironmental Engineering,* vol. 123, no. 7, pp. 663-370, 1997.

[25] E. G. Fernando, J. Oh, D. Ryu and S. Nazarian, "Consideration of Regional Variations in Climatic and Soil Conditions in the Modified Triaxial Design Method," National Technical Information Service, Springfield, VA, 2008.

[26] G. R. McKeen, "Design and Construction of Airports Pavements on Expansive Soils," International Technical Information Service, Sprinfield, VA, 1976.

[27] S. Saha, N. Hariharan, F. Gu, X. Luo, D. N. Little and R. L. Lytton, "Development of a Mechanistic-Empirical Model to Predict Equilibrium Suction for Subgrade Soil," *Journal of Hydrology,* vol. 575, 2019.

[28] Texas Transportation Institute - Materials and Pavements, "Flexible Pavement Design in TxDOT," Texas Department of Transportation, 2020.

[29] T. Scullion, "Pavement Design and Rehabilitation Training Schools," Texas Transportation Institute, 2021.

[30] H. Nabizadeh, R. V. Siddharthan, E. Y. Hajj, M. Nimeri and S. Elfass, "Validation of the Subgrade Shear Strength Parameters Estimation Methodology Using Light Weight Deflectometer: Numerical Simulation and Measured Testing Data," *Transportation Geotechnics,* vol. 21, 2019.

[31] S. a. F. Mulyawati, "Comparative Study of the Use of FWD and LWD for Flexible Pavement Evaluation," *J. Phy.: Conf. Ser.,* no. 1517 012031, 2020.

[32] N. Siddiki, "2012 Road School Light Weight Deflectometer (LWD)," Indiana Department of Transportation.

[33] M. Nazzal, M. Abu-Farsakh, K. Alshibh and L. Mohammed, "Evaluating the Potential Use of a Portable LFWD for Characterizing Pavement Layers and Subgrades," *Geotechnical Engineering for Transportation Projects,* 2004.

[34] D. Kuttah, "Determining the Resilient Modulus of Sandy Subgrade Using Cyclic Light Weight Deflectometer Test," *Transportation Geotechnics,* vol. 27, 2021.

[35] V. M. Garcia and J. Robinson, "Application of Light Weight Deflectometer to Assess Structural Competency of Nontraditional Airfield Pavements during Contingency Aircraft Operations," in *13th TRB International Conference on Low Volume Roads*.

[36] FAARFIELD Software Help , *Introduction to FAARFIELD,* Federal Aviation Administration.

[37] Federal Aviation Administration, *Advisory Circular: Airport Pavement Design and Evaluation,* Federal Aviation Administration, 2021.

[38] I. Kawa, "Pass-to-Coverage Computation for Arbitrary Gear Configuration in the FAARFIELD Program," National Technical Information Service, Springfield, VA, 2012.

[39] Texas General Land Office, *Texas Coastal Zone,* Texas General Land Office.

[40] National Aeronautics and Space Administration, "Data & Applications Online," April 2017. [Online]. Available: http://www.ciesin.org/documents/lecz-final.pdf. [Accessed 2022].

[41] AirNav, "Airport Information," AirNav, LLC, 2022. [Online]. Available: https://www.airnav.com/airports/. [Accessed 15 August 2022].

[42] General Aviation News Staff, "Top 10 Best Selling Business Jets in 2020," General Aviation News, 11 March 2021. [Online]. Available: https://generalaviationnews.com/2021/03/14/top-10-best-selling-business-jets-in-2020/. [Accessed 15 August 2022].

[43] General Aviation News Staff, "Top 10 Best Selling Piston Airplanes in 2020," General Aviation News, 11 March 2021. [Online]. Available: https://generalaviationnews.com/2021/03/14/top-10-best-selling-piston-airplanes-in-2020/. [Accessed 15 August 2022].

[44] General Aviation News Staff, "Top 10 Best Selling Turboprops in 2020," General Aviation News, 15 March 2021. [Online]. Available: https://generalaviationnews.com/2021/03/15/top-selling-turboprops-in-2020/. [Accessed 15 August 2022].

[45] Victoria Regional Airport, "Flights from Victoria to Houston," 8 June 2022. [Online]. Available: https://flyvictoriatx.com/. [Accessed 15 August 2022].

[46] Midland International Air and Space Port, "Photo Gallery," [Online]. Available: https://www.flymaf.com/gallery.aspx. [Accessed 15 August 2022].

[47] Scholes International Airport, "Photo Archives," 2022. [Online]. Available: https://www.galvestonairport.com/photo-archives. [Accessed 15 August 2022].

[48] American Airlines, "Planes - Travel Information - American Airlines," 2022. [Online]. Available: https://www.aa.com/i18n/travel-info/experience/planes/planes.jsp. [Accessed 15 August 2022].

[49] Airfleets.net, "Southwest Airlines Fleet Details," 2022. [Online]. Available: https://www.airfleets.net/flottecie/Southwest%20Airlines.htm. [Accessed 15 August 2022].

[50] United Airlines, "United Airlines Fleet and Aircraft Information," 2022. [Online]. Available: https://www.united.com/ual/en/us/fly/travel/inflight/united-airlines-fleet.html. [Accessed 15 August 2022].

[51] Texas Department of Transportation, *Structural Data in PA Falling Weight Deflectometer and Traffic Speed Deflectometer,* Texas Department of Transportation.

[52] United States Department of Agriculture Soil Science Division Staff, Soil Survey Manual, United States Department of Agriculture, 2017.

[53] Natural Resources Conservation Service, "Web Soil Survey," United States Department of Agriculture, [Online]. Available: https://websoilsurvey.sc.egov.usda.gov/App/HomePage.htm.

APPENDIX A

THE TEXAS COASTAL ZONE

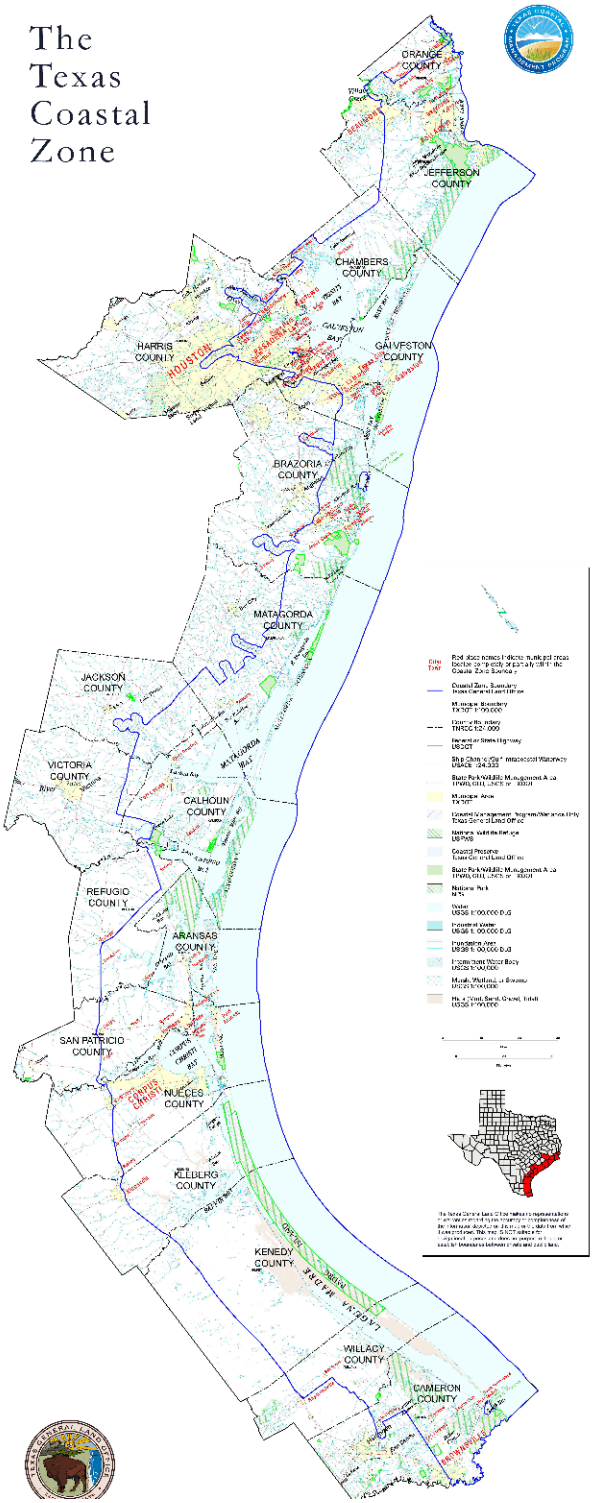

APPENDIX B

PERCENT REDUCTION IN SINGLE USE SWL THROUGHOUT THE FLOOD SIMULATION.

Airport		Normal Conditions	Completely Inundated	Dry Base	Inundated Subgrade
Anahuac	**SWL (1,000 lbs.)**	180.5	140	145	140
	% Reduction	-	22	20	22
Bay City	**SWL (1,000 lbs.)**	180	139	160	143
	% Reduction	-	23	11	21
Brenham	**SWL (1,000 lbs.)**	230	158	189	185
	% Reduction	-	31	18	20
Caldwell	**SWL (1,000 lbs.)**	240	184	190	192
	% Reduction	-	23	21	20
Houston SW	**SWL (1,000 lbs.)**	225	148	158	156
	% Reduction	-	34	30	31
La Porte	**SWL (1,000 lbs.)**	172	158	162.5	164
	% Reduction	-	8	6	5
Orange	**SWL (1,000 lbs.)**	328	260	270	-
	% Reduction	-	21	18	-
Port Lavaca	**SWL (1,000 lbs.)**	282.5	200	207	210
	% Reduction	-	29	27	26
Rockdale	**SWL (1,000 lbs.)**	98	78	78	-
	% Reduction	-	20	20	-
Winnie	**SWL (1,000 lbs.)**	120.5	93	95	98
	% Reduction	-	23	21	19

APPENDIX C

TESTED AIRPORT GEOTECHNICAL INFORMATION

Airport	AASHTO Group Classification	Plasticity Index (PI)	Ksat (in/hr)	Ksat Class	Drainage Class
Anahuac	A-7-6	41.3	0.057	Moderately Low	Somewhat Poorly Drained
Bay City	A-6	32	0.048	Moderately Low	Somewhat Poorly Drained
Brenham	A-7-5	39	0.030	Moderately Low	Somewhat Poorly Drained
Caldwell	A-6	33.5	0.276	Moderately High	Moderately Well Drained
Houston SW	A-7-6	40	0.013	Low	Moderately Well Drained
La Porte	A-7-6	40	0.013	Low	Moderately Well Drained
Orange	A-6	17.4	0.085	Moderately Low	Poorly Drained
Port Lavaca	A-7-5	31.9	0.030	Moderately Low	Moderately Well Drained
Rockdale	A-2-4	11.3	2.233	High	Moderately Well Drained
Winnie	A-7-6	53.5	0.029	Moderately Low	Poorly Drained